Material Science and Technology Division

Heavy Vehicle Propulsion Materials Program
Quarterly Progress Report for
January through March 2007

D. R. Johnson
Technical Project Manager

Prepared for
U.S. Department of Energy
Assistant Secretary for Energy Efficiency and Renewable Energy
Office of FreedomCAR and Vehicle Technologies Program
VT 05 01 020

Prepared by the
OAK RIDGE NATIONAL LABORATORY
Oak Ridge, Tennessee 37831-6066
Managed by
UT-Battelle, LLC
for the Department of Energy
Under contract DE-AC05-00OR22725

CONTENTS

Project 18518 – Materials for High Efficiency Engines

*Lightweight Valve Train Materials (*Caterpillar)

Mechanical Reliability of PZT Piezo-Stack Actuators for Fuel Injectors (ORNL)

Friction and Wear Reduction in Diesel Engine Valve Trains (ORNL)

NDE of Diesel Engine Components (Argonne)

Project 18519 – Materials for Control of Exhaust Gases and Energy Recovery Systems

Advanced Cast Austenitic Stainless Steels for High Temperature Components, CRADA with Caterpillar (ORNL)

Development of Materials Analysis Tools for Studying SCR Catalysts, CRADA with Cummins (ORNL)

Durability and Reliability of Ceramic Substrates for Diesel Particulate Filters, CRADA with Cummins (ORNL)

Catalysis by First Principles - Can Theoretical Modeling and Experiments Play a Complimentary Role in Catalysis? (ORNL)

Project 18865 – Materials by Design

Characterization of Catalyst Microstructures and Deactivation Mechanisms (ORNL)

Life Prediction of Diesel Engine Components (ORNL)

Powder Processing of Nanostructured Alloys Produced by Machining (Purdue)

Modeling of Thermoelectrics (ORNL)

Lightweight Valve Train Materials

Nathaniel S. L. Phillips
Caterpillar Inc.

Introduction

Valve train components in heavy-duty engines operate under high stresses and temperatures, and in severe corrosive environments. In contrast, the valve train components in the light-duty engine market require cost-effective reliable materials that are wear resistant and lightweight in order to achieve high power density. For both engine classes, better valve train materials need to be identified to meet market demand for high reliability and improved performance, while providing the consumer lower operating costs.

Advanced ceramics and emerging intermetallic materials are highly corrosion and oxidation resistant, and possess high strength and hardness at elevated temperatures. These properties are expected to allow higher engine operating temperatures, lower wear, and enhanced reliability. In addition, the lighter weight of these materials (about 1/3 of production alloys) will lead to lower reciprocating valve train mass that could improve fuel efficiency. This research and development program is an in-depth investigation of the potential for use of these materials in heavy-duty engine environments.

The overall valve train effort will provide the materials, design, manufacturing, and economic information necessary to bring these new materials and technologies to commercial realization. With this information, component designs will be optimized using computer-based lifetime prediction models, and validated in rig bench tests and short-and long-term engine tests.

Program Overview

Information presented in this report is based on previous proprietary research conducted under Cooperative Agreement DE-FC05-97OR22579.

Ceramic Materials:

Silicon nitride materials have been targeted for valve train materials in automotive and diesel industries since the early 1980's. Some silicon nitride (Si_3N_4) material grades have reached a mature level of materials processing, capable of being implemented into production. Commercial realizations have been reported in both automotive and diesel valve trains, with large-scale production underway. The Si_3N_4 valve train components in production are used in high rolling contact stress applications and have exhibited superior wear resistance and longevity.

Intermetallic Materials:

Titanium aluminide (TiAl) based intermetallics retain their strength at elevated temperature and are highly corrosion-resistant. They are lightweight and possess high fracture toughness. These alloys are actively being investigated for several aerospace and automotive applications.

Summary

The primary focus of this quarter was the residual stress analysis of the machined Kyocera SN235P Si_3N_4 test rods and to start Phase #3 engine exposure of the lightweight valves on the Caterpillar natural gas G3406 genset. A trip to Oak Ridge National Lab from March 19-30 was made to perform the residual stress measurements at the High Temperature Materials Laboratory User Center and to

prepare the G3406 test engine for the 2nd 500 hours of engine exposure as outlined in the 1Q07 DOE Adv Valve Report.

This quarterly report will document the preliminary results from the residual stress test measurements and will update the progress of testing on the genset engine. Also, the plans for next quarter will be outlined.

Residual Stress Tests *- HTML User Proposal No. 2003-058 "Effect of Machining Procedures on the Strength of Ceramics for Diesel Engine Exhaust Valves"*

The aforementioned user proposal was developed in 2004 to develop cost effective machining processes for ceramic components resulting in optimal performance and extended life and reliability. The machining conditions and results of the Weibull moduli and characteristic strength tests of machined Kyocera SN235P Si_3N_4 test rods are outlined in FY04 DOE Adv Valve Annual Report. A wide range of Weibull moduli were reported for the different machining techniques; however, the characteristic strengths were all very similar. Therefore, it was decided that experiments should be done to determine if differences in residual stresses as a result of the machining processes were causing the variation in moduli.

A test matrix was setup to compare the highest to lowest Weibull moduli test specimens, as outlined in Table 1. Measurements were to be taken in the axial, radial, and hoop directions with the XRD-PTS Rotating Anode. Thus far, only the first four samples have been tested. The machining information from these four samples is presented in Table 2. The surface finishes of these samples were laser scattered and optically imaged, as shown in Figure 1.

After finding little stress in these samples by employing the conventional method of x-ray diffraction (XRD) due to averaging effects, it was determined that grazing incidence x-ray diffraction (GIXD) should be used to determine the stress at the near surface (approximately first 10 μm). However, the results from GIXD are more qualitative than quantitative and will only give an approximate value of the actual residual stress. Figure 2 shows the relative comparison of the samples listed in Table 2 as a result of the GIXD analysis. There is a steep stress gradient in the first few microns of the surface. As the depth increases, the stress levels off. The samples which were finished machined and had the highest Weibull moduli, 2A and 2B, showed the highest compressional stresses at the surface. This suggests that the high compressional stresses prevent crack initiation in the finished samples better than the rough samples. The finished machining shears the surface more than the rough grinding, creating more of a smeared, deformed surface (see Figure 1). This suggests that the finished machining more uniformly distributes the surface flaws, since Weibull modulus is a measure of variance. It is currently being determined if tests outlined in the test matrix should continue based on these results.

G3406 Genset Engine Exposure – Phase #3

A new, instrumented production head was donated to NTRC for the use on the G3406 genset test engine in February. The new head was equipped with thermocouples to measure the exhaust seat temperatures to assist with the understanding of how ceramics and intermetallics affect the combustion and valve temperatures. Holes were also drilled in the head for pressure transducers to determine if the combustion cycle was performing properly. However, due to unexpected

complications, the new head was deemed unusable for Phase #3 testing. The valves from Phases #1 and 2 and new seat inserts were reassembled into the old head and made ready for testing.

The changes to the valve configuration in the head for Phase #3 were performed as outlined in 1Q07 DOE Adv Valve Report. The new configuration of valves is presented in Figure 3. Preliminary testing showed that the engine could run at rated conditions (235 kW) instead of half rated, as a result of the changes. However, due to some unexpected mechanical failures of the pressure transducers/charge amplifier, the completion of Phase #3 was delayed until next quarter.

Next Steps

The GIXD residual stress measurements of the Si_3N_4 machined cylindrical tests specimens will continue. Upon completion of the test matrix, results will be quantified to determine which machining technique is best for Kyocera SN235P valves. Further studies are also planned to analyze the residual stress with Raman spectroscopy and nano-indentation. Initial plans have been set to do a similar machining study on Ceradyne 147-31N Si_3N_4 machined cylindrical rods.

Phase #3 on the genset will be completed once all of the mechanical malfunctions have been corrected. After the engine is run for another 500 hours, all valves will be removed, inspected and prepared for destructive testing. By performing fast fracture tests on valves that have accumulated 0, 500, 1000 hours of engine time, the effect of engine aging on the materials' retained strength will be examined. Along with combustion dynamics and fuel consumption measurements, this data will enable the team to quantify the performance gains and durability of Si_3N_4 and TiAl valves in a heavy-duty engine environment.

Table 1. Test matrix for residual stress tests

Sample #	Machining Rank*	XRD Scans - 1 Spot Axial	Hoop	Radial
2A	1	Y	Y	Y
4A	12	Y	Y	Y
2B	1	Y	Y	Y
4B	12	Y	Y	Y
Do we see a difference? Y: Continue, N: End Testing				
12A	2	Determine if all 3 directions are necessary based on data. Perform the minimum number of directions as necessary.		
10A	11			
12B	2			
10B	11			
Do we see a difference? Y: Continue, N: End Testing				
7A	3	Determine if all 3 directions are necessary based on data. Perform the minimum number of directions as necessary.		
3A	10			
7B	3			
3B	10			

* Machining Rank: 1=Best sample, 12=Worse sample

Table 2. Machining processes for samples in test matrix

Sample ID	Machining Condition
2A	Finished
4A	Rough
2B	Finished
4B	Rough

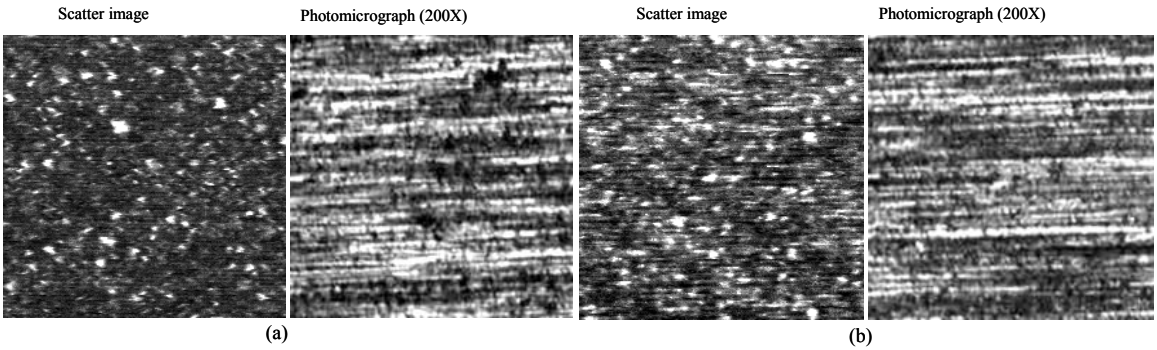

Figure 1. (a) Finished and (b) rough machined Si_3N_4 specimens

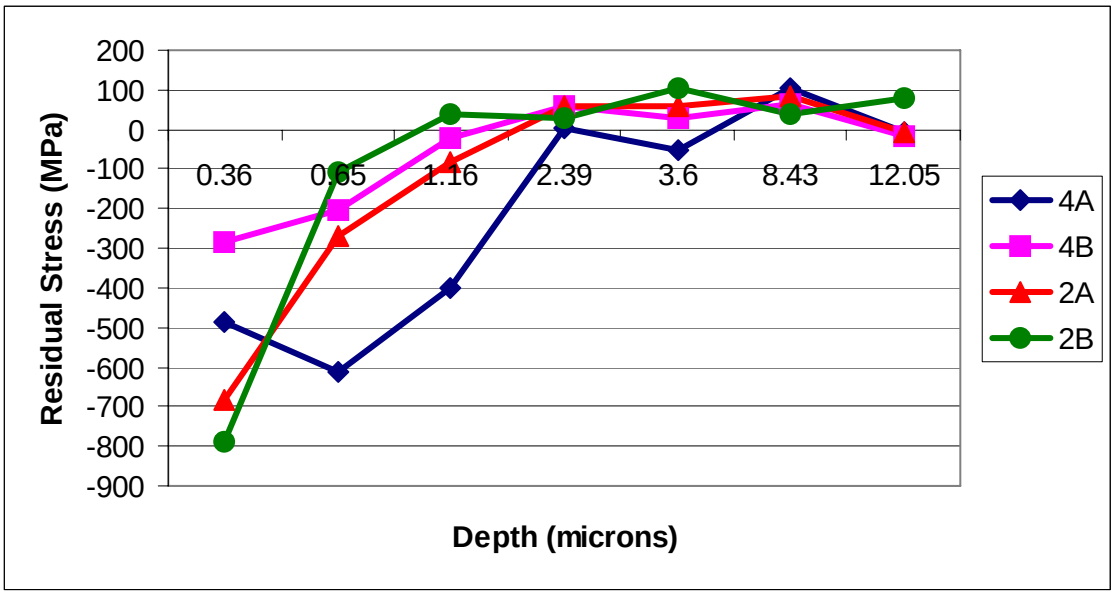

Figure 2. Relative GIXD residual stress results as a function of sample depth for machined SN235P Si_3N_4 test rods

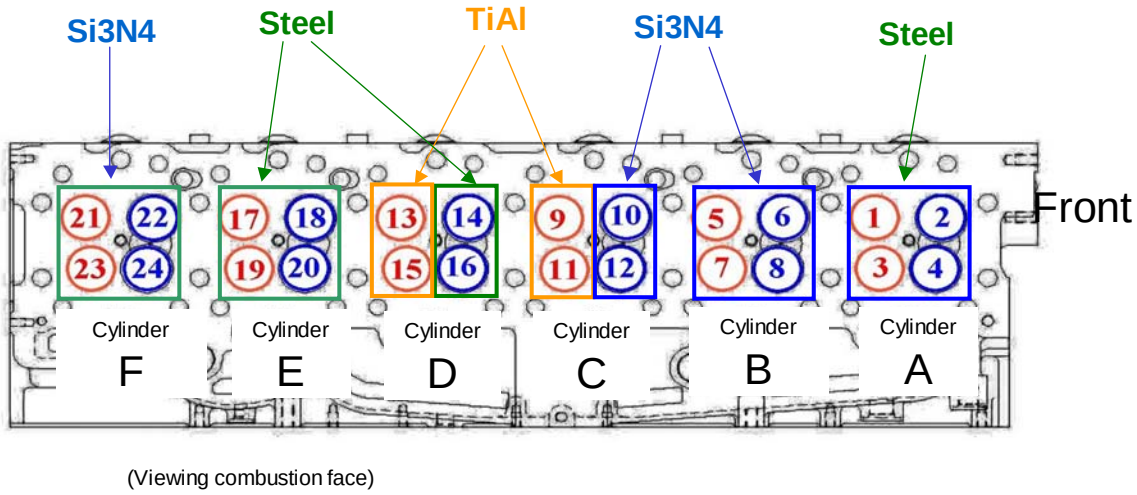

Figure 3. Valve arrangement for Phase #3

Mechanical Reliability of PZT Piezo-Stack Actuators for Fuel Injectors

A. A. Wereszczak and H. Wang
Ceramic Science and Technology (CerSAT)
Oak Ridge National Laboratory

Objective/Scope

The use of piezoelectric stack actuators as diesel fuel injectors has the potential to reduce injector response time, provide greater precision and control of the fuel injection event, and lessen energy consumption (e.g., for use in homogeneous charge compression ignition, HCCI, engines). Though piezoelectric function is the obvious primary function of lead zirconate titanate (PZT) ceramic stacks for fuel injectors, their mechanical reliability can be a performance and life limiter because PZT is both brittle, lacks high strength, and may exhibit fatigue (i.e., slow crack growth) susceptibility. That brittleness and relatively low strength can be overcome with proper design though. This project combines in-situ micromechanical testing, microstructural-scale finite element analysis, probabilistic design sensitivity, and structural ceramic probabilistic life prediction methods to systematically characterize and optimally design PZT piezoelectric stack actuators that will enable maximized performance and operational lifetime.

Technical Highlights

Assembly of the piezoactuator test facility was completed during the present reporting period. The setup is shown in Fig. 1. The whole load train is capable of applying a static compressive load to the piezostack actuator through dead-weight loading (plans exist in FY08 to replace this with a loading actuator capable of applying a monotonically increasing force for accelerated testing). A piezostack actuator is mounted between parallel (horizontal) metal plates having two non-contact capacitance gages mounted on them. Semi-articulating (electrically insulating) silicon nitride push rods apply the static compressive force on the piezostack actuator. Even though a dead weight is used to apply a static load, a load cell is positioned in the load train to enable load measurement throughout cyclic loading. Customized software (MTIC, Oak Ridge, TN) is used to excite a high-voltage, high frequency amplifier that in turn drives the piezostack actuator. Additionally, that same software monitors applied voltage and displacement signals from the capacitance gages, and is programmable to take periodic “snapshots” of the data during high frequency testing. Voltages and displacement signals are then used to calculate electric fields, amount of charge, charge densities, and strains (see Fig. 2).

Piezostack actuators from different manufacturers are now undergoing evaluation as a function of static compressive stress, applied voltage, and frequency.

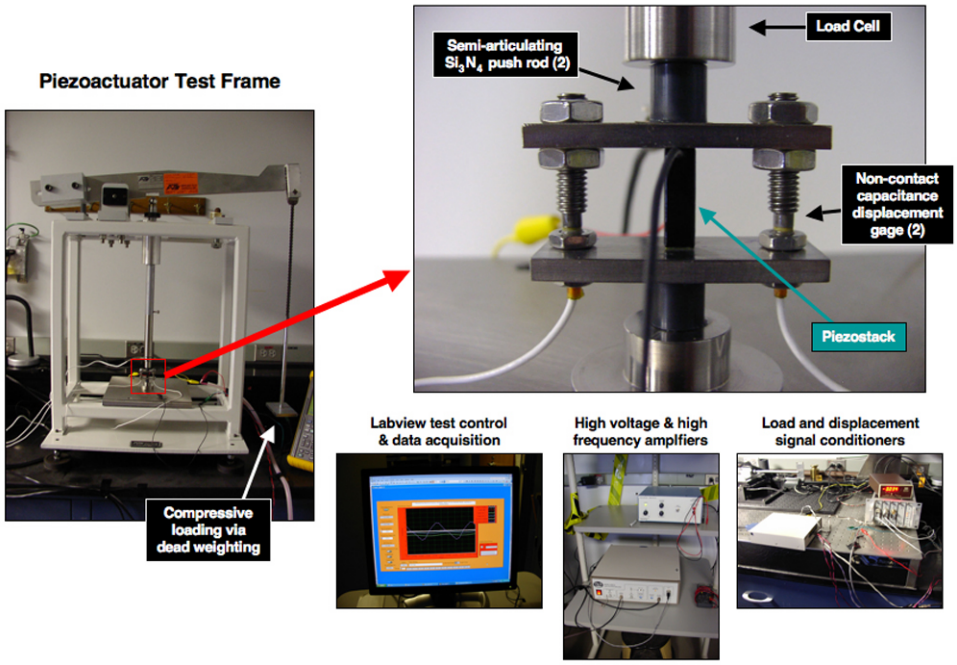

Figure 1. Piezoactuator test frame is shown at the left with an enlargement of the test assembly (with mounted piezoactuator) shown in the upper right. Subcomponents shown at lower right.

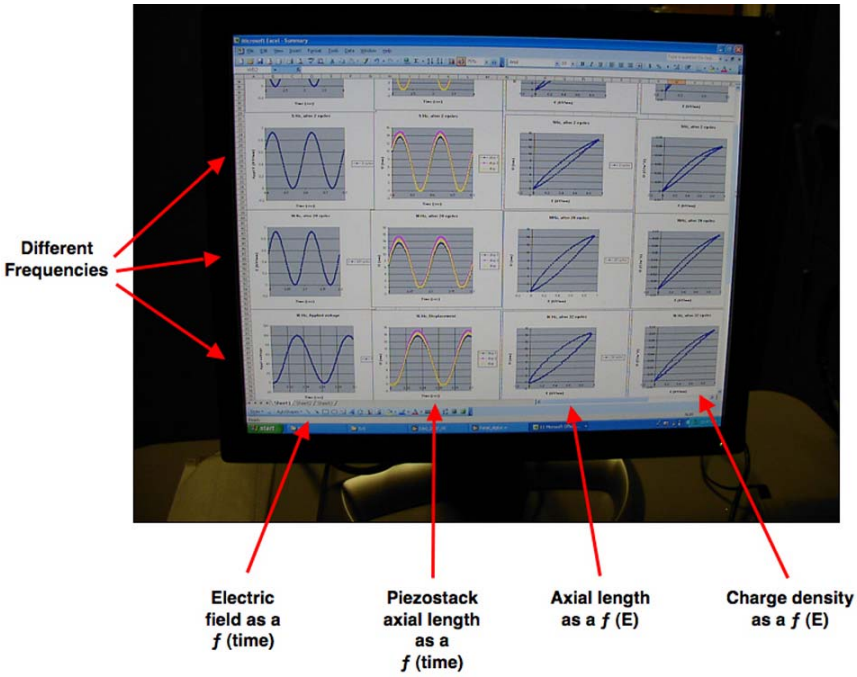

Figure 2. Examples of the "snapshot" functions that can be analyzed during high frequency cycling.

Our initial testing is examining changes in hysteresis behavior as a function of the number of cycles. One example of this is shown in Fig. 3. For this test, a piezostack actuator was subjected to 30 MPa of static compressive stress and 10 Hz cycling between 0 and 100 volts. Initial response is compared with those after 1 million (M), 5M, 16M, 26M, and 38M cycles.

Methods are now being assessed to enable accelerated testing of these piezostack actuators. Additional, the introduction of temperature-controlled testing is being pursued.

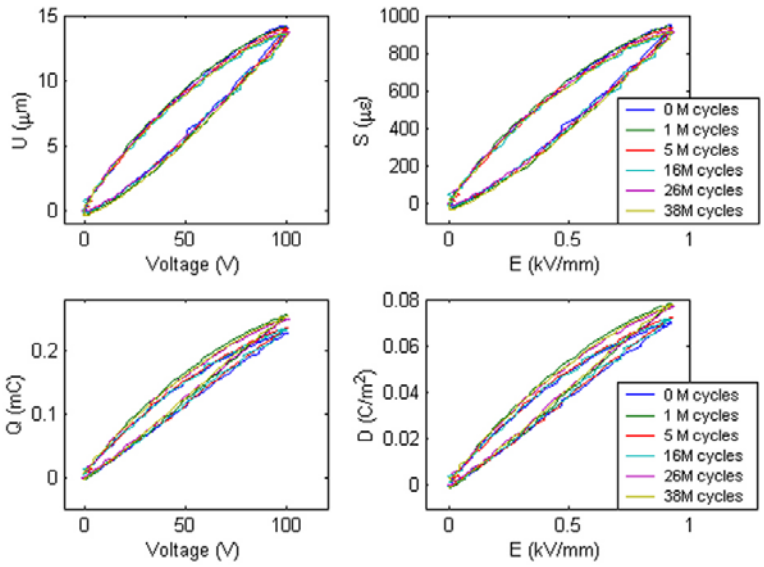

Figure 3. Displacement (U) versus applied voltage, strain (S) versus electric field (E), charge (Q) versus voltage, and charge density (D) versus electric field under a compressive stress of 30 MPa and a 10 Hz frequency as a function of total number of cycles.

Status of FY 2007 Milestones

Establish piezoactuator reliability test facility. [09/07] *On schedule.*

Communications/Visits/Travel

Separate discussions held with Caterpillar, EPCOS, Noliac, and Penn State University.

Publications

H. Wang and A. A. Wereszczak, "Effects of Electric Field on the Biaxial Strength of Poled PZT," in press, *Ceramic Engineering and Science Proceedings, 2007.*

References

None.

Friction and Wear Reduction in Diesel Engine Valve Trains

Peter Blau
Oak Ridge National Laboratory

Objective/Scope

The objective of this effort is to enable the selection and use of improved materials, surface treatments, and lubricating strategies for value train components in energy-efficient diesel engines. Depending on engine design and operating conditions, between 5 and 20% of the friction losses in an internal combustion engine are attributable to the rubbing between valve train components. Wear and consequent leaks around valve seats can reduce cylinder pressure and engine efficiency. Contacting surfaces in the valve train include the valve heads, seats, tappets, guides, and stems. This effort is designed to address key rubbing interfaces within the valve train where there are opportunities to employ advanced materials and surface treatments to reduce friction and save energy.

A two-pronged, interdisciplinary approach is planned to address both materials and lubrication-related aspects. The first task concerns the design and construction of a laboratory testing apparatus to simulate the thermal, chemical, and mechanical contact environment characteristic of valves and valve seats. The second task involves improving the performance of the valve stems as they oscillate within the valve guides. Task one is under way.

Technical Highlights

Completion of a High-Temperature Valve Material Testing System. The construction and design features of a controlled-environment, repetitive-impact system were described in the previous quarterly report. The new High-Temperature Repeated Impact (HTRI) apparatus is now available to investigate the durability of candidate exhaust value materials, to identify their primary modes of surface damage and to develop guidance for the selection of new bulk materials, coatings, and surface treatments for use in engines that burn a variety of fuels.

Preliminary tests were conducted at 800° C in air to check the alignment of the specimens and to become familiar with the kinds of surface damage that might be produced using this facility. A production diesel engine exhaust valve with a 45 degree seat angle was used for these experiments, but the stainless steel counterface material was not typical of valve seat alloys. Rather, commercial and experimental valve seat alloys are in the process of being obtained from a manufacturer.

Low magnification photomicrographs in Figure 1 show contact damage on the valve head after 20,000 impacts when the valve is allowed to rotate without constraint in its holder. Valves are known to rotate in actual engines and the combination of sliding and impact makes it more challenging to model the surface degradation process. Features indicate clear evidence for adhesive transfer ('micro-welding'), sliding with plastic deformation, and scoring. The valve holder also has the capability to pin the valve specimen in one position in order to enable repetitive impact without rotation.

.

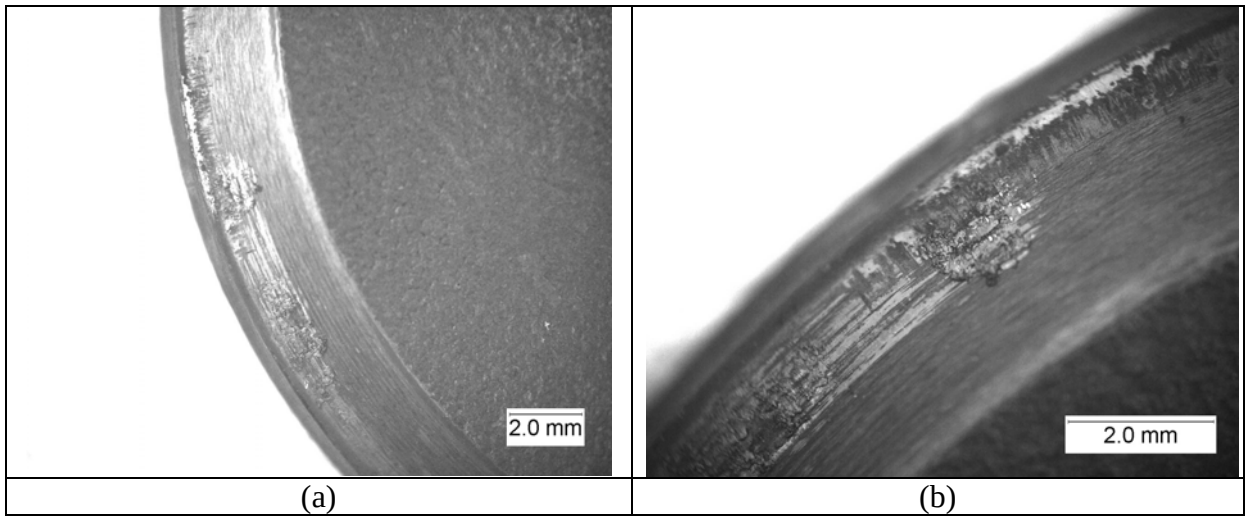

Figure 1. Surface damage on a production diesel engine exhaust valve tested in the HTRI apparatus. (a) 20,000 repetitive impacts with unrestrained rotation in air at 800°C. (b) Indications of material transfer and micro-welding are clearly visible.

Progress on this project has been slowed due to the reduced 2007 budget, but discussions with suppliers and engine companies continue with the aim of obtaining seat materials and samples of worn valves from diesel engines when additional support becomes available.

Future Plans

1) Obtain conventional seat materials for testing.

2) Work with an engine manufacturer to obtain samples of diesel engine valves that were run in fired engines and compare wear damage to that generated in the HTRI.

Travel

None

Status of Milestones

1) Complete first matrix of tests to compare traditional and advanced valve/valve seat materials at high temperature, in controlled-atmosphere, and with repetitive impact conditions. Submit report or journal article on the results. **(03/07) –** *completion delayed due to changes in funding.*

2) Prepare an analysis of the basic mechanisms that operate as valve/valve seat materials degrade in service and correlate them with basic material properties and metallurgical structure. Submit report or journal article describing the analysis. **(09/07)**

Publications and Presentations

None.

NDE of Diesel Engine Components

J. G. Sun and N. Phillips*
Argonne National Laboratory
***Caterpillar, Inc.**

Objective/Scope

Emission reduction in diesel engines designated to burn fuels from several sources has lead to the need to assess ceramic valves to reduce corrosion and emission. The objective of this work is to evaluate several nondestructive evaluation (NDE) methods to detect defect/damage in structural ceramic valves for diesel engines. One primary NDE method to be addressed is elastic optical scattering. The end target is to demonstrate that NDE data can be correlated to material damage as well as used to predict material microstructural and mechanical properties. There are two tasks to be carried out: (1) Characterize subsurface defects and machining damage in flexure-bar specimens of NT551 and SN235 silicon nitrides (Si_3N_4) to be used as valve materials. Laser-scattering studies will be conducted at various wavelengths using a He-Ne laser and a tunable-wavelength solid-state laser to optimize detection sensitivity. NDE studies will be coupled with examination of surface/subsurface microstructure and fracture surface to determine defect/damage depth and fracture origin. NDE data will also be correlated with mechanical properties. (2) Assess and evaluate surface and subsurface damage in Si_3N_4 and TiAl valves to be tested in a bench rig and in an engine. All valves will be examined at ANL prior to test, during periodic scheduled shut downs, and at the end of the planned test runs.

Technical Highlights

Work during this period (January-March 2007) focused on developing the cross-polarization confocal microscopy system for high-resolution 3D imaging of subsurface cracks in silicon-nitride ceramics.

1. Laser-Scatter NDE Evaluation of Engine-Tested Valves

The 14 Si_3N_4 and TiAl valves that have been tested in the natural gas G3406 generator set at the NTRC for 500 hours will be installed for the third and last phase of 500-hr testing. It is expected that this 500-hr engine test will be conducted in the next reporting period. NDE inspection of these valves after this test will be performed and results will be presented in the next period.

2. Development of a Cross-Polarization Confocal System for Measurement of 3D Subsurface Microstructure in Silicon Nitride Ceramics

In our January-March 2006 report we described the development of a cross-polarization confocal microscopy system that is capable of imaging detailed 3D subsurface microstructure in translucent silicon-nitride materials. Preliminary tests demonstrated that, with a moderate 40X objective lens at an optical wavelength of 633 nm, the system has an axial (depth) resolution of ~2 µm and a lateral resolution of ~0.6 µm. Further improvement in spatial resolution was investigated in this period. For a diffraction-limited lens, the focused light spot has a diameter of $D = 1.22\lambda / NA$ in the focal plane and an axial length of $Z = 4\lambda/(NA)^2$, where λ is light wavelength and *NA* is the numerical aperture of the lens. The focused spot size, which represents the spatial resolution, is therefore determined by the *NA* of the lens. High spatial resolution can be achieved by using high-magnification lenses that have high *NA* values. In this

period, we have obtained a 63X objective lens with *NA* = 0.75 (*NA* = 0.6 for the 40X lens). The axial resolution, which is lower than the lateral resolution for confocal systems, is normally determined by scanning a mirror surface. The mirror is scanned in the x-z plane where x-direction is parallel to the mirror surface and z-direction is normal to the mirror surface. Figure 1 shows x-z scan images obtained using the 40X and 63X objective lenses. The scan-step size in both x and z directions was 0.1 μm. A line profile in the z-direction from each image in Fig. 1 is plotted in Fig. 2, where the intensity is normalized to be 1 at the mirror surface. From the measured-intensity profile, an axial resolution parameter, commonly defined as the full-width at half-maximum (FWHM), can be determined. FWHM is 2 μm for the 40X lens and 1.3 μm for the 63X lens; these numbers are consistent with the change of *NA* values between the two lenses. Based on this result, a 100X lens with *NA* = 0.9 will provide an axial FWHM resolution of 0.9 μm in air, which is likely the highest resolution ever achieved by an optical method. Such a lens has been ordered and is expected to be received in the next period.

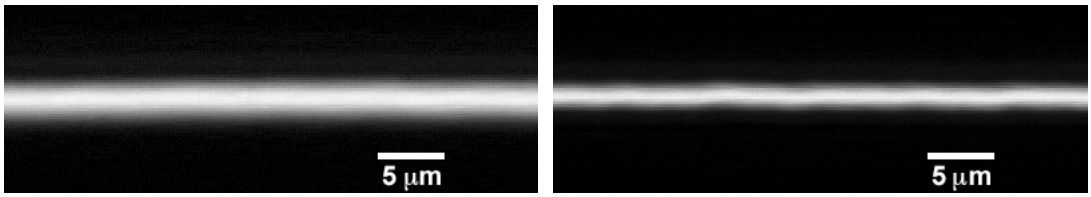

(a) (b)

Fig. 1. Scan images of a mirror surface with (a) 40X and (b) 63X objective lens.

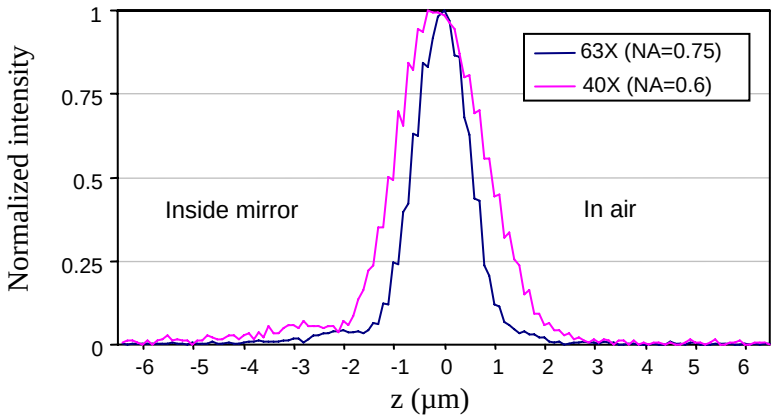

Fig. 2. Axial intensity profiles obtained from the scan images in Fig. 1.

A NT551 silicon nitride specimen with known subsurface C cracks was tested using the confocal setup with the 63X objective lens. Figure 3 shows a lateral (plane) scan image of a damaged region with two C cracks. Higher scatter intensity is observed from both C cracks as well as from many individual material defects (likely porous pores). To examine the crack angle and depth within the subsurface, five cross-sectional scans, spaced at 40-μm distances from each other as marked as Slices 1-5 in Fig. 3, were performed. The 5 cross-sectional scan images are shown in Fig. 4, with the inside of the material on the top and the specimen surface at the bottom in each image of 1 mm x 0.04 mm size. The extension of the C cracks is clearly visualized in these cross-sectional images. However, as shown in the enlarge image in Fig. 5, which is taken from the marked region in Fig. 4, the scan (horizontal) lines are not well aligned in the vertical direction. This was due to the poor accuracy of the current scan stage, which could have a

maximum error of >3 µm. A new scan stage with a specified spatial accuracy of 0.2 µm has been obtained and will be implemented into the system in the next period. Another issue with the current system is a shallow detection depth. From Fig. 4, the detection depth is estimated to be about 30 micron for the NT551 material at the laser wavelength of 633 nm. The depth of optical penetration can be increased with longer optical wavelengths. Work will be continued to utilize an infrared 850-nm wavelength to improve the detection depth.

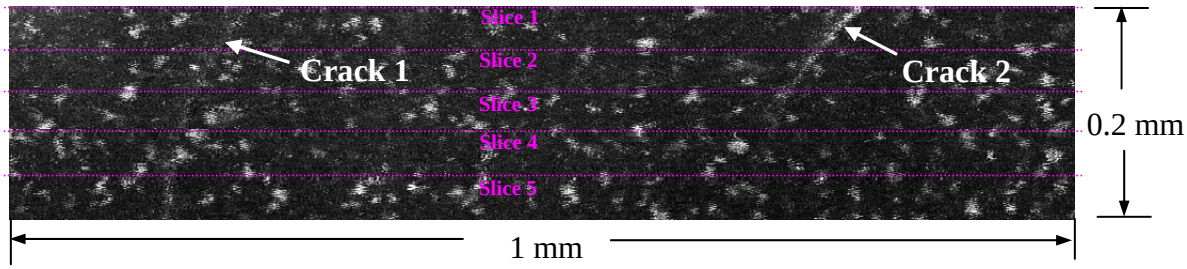

Fig. 3. Plane confocal-scan image of a NT551 silicon nitride specimen with two C cracks.

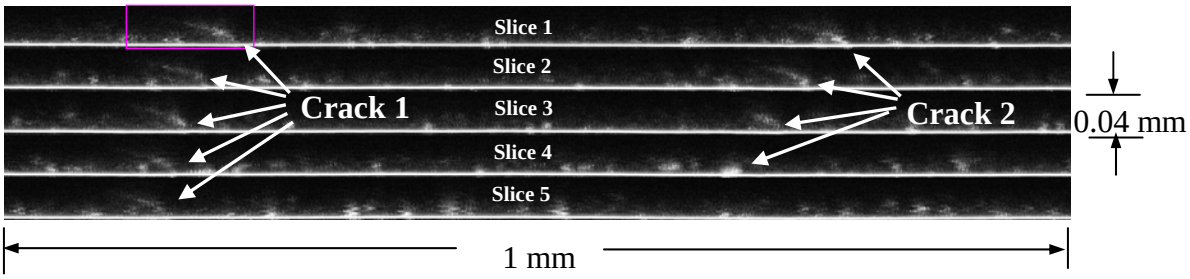

Fig. 4. Five cross-sectional confocal-scan images along slice lines 1-5 as indicated in Fig. 3.

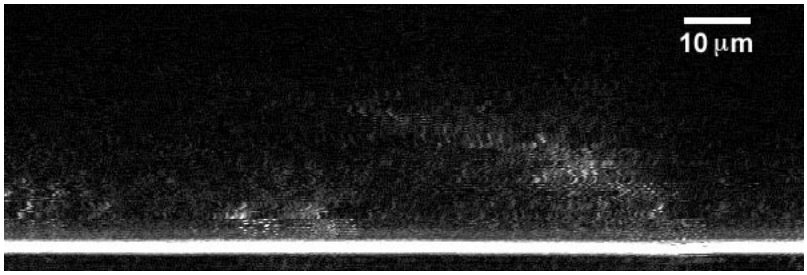

Fig. 5. An enlarged region from a cross-sectional confocal-scan image as marked in Fig. 4.

Status of Milestones

Current ANL milestones are on schedule.

Communications/Visits/Travel

1. J.G. Sun attended the 31st Int. Cocoa Beach Conf. & Exposition on Advanced Ceramics and Composites held in January 21-26, 2007 in Daytona Beach, FL, and presented a paper

entitled "Nondestructive Evaluation of Silicon-Nitride Ceramic Valves from Engine Duration Test," co-authored by J.G. Sun, J. S. Trethewey, N. Phillips, N. N. Vanderspiegel, and J. A. Jensen.

2. J.G. Sun visited Caterpillar Inc. on February 21, 2007 to discuss project issues.

Problems Encountered

None this period.

Publications

None this period.

Advanced Cast Austenitic Stainless Steels for High Temperature Components

P. J. Maziasz, John P. Shingledecker, and N. D. Evans
Oak Ridge National Laboratory

M. J Pollard
Caterpillar, Inc.

Objective/Scope

This is the 2nd ORNL CRADA project with Caterpillar. This CRADA project is focused on commercialization of the new CF8C-Plus cast austenitic stainless steel, which was developed during the first ORNL/CAT CRADA. CF8C-Plus stainless steel is a cost-effective material upgrade for much more performance, durability and temperature capability relative to current heavy-duty diesel engine exhaust components made from SiMo ductile cast iron. In FY2005, this project completed the initial properties data base needed for alternate materials selection, and component design or redesign, including fatigue, thermal fatigue, and creep, and studies of aged materials. In FY2006, longer term creep-testing and fatigue studies at much lower frequencies were completed, together with new tests directly related to specific new component applications, like turbocharger housings. This CRADA (Cooperative Research and Development Agreement) project (ORNL02-0658) was extended beyond the initial 3-year term last year, and will be completed in July, 2007. Requests for more detailed information on this project should be made directly to Caterpillar, Inc.

Highlights

Caterpillar, Inc.

Caterpillar and ORNL are working together to obtain an ASTM alloy designation for CF8C-Plus stainless steel. The Caterpillar Regeneration System (CRS) components are currently being produced from CF8C-Plus steel for on-road engine applications begin in 2007. Trial licenses for several commercial applications are in the final negotiating stages with Caterpillar.

ORNL

Stainless Foundry & Engineering (SF&E, one of the three current trial-licensees) completed successful welding and testing of CF8C-Plus for the ASTM Weld Procedure Qualification. SF&E (Ron Bird) is preparing the final package for approving a new alloy grade (HG10MNN) for the ASTM A297 Specification. ORNL has begun tensile and creep testing of step castings of both CF8C-Plus and –Plus Cu/W produced by SF&E to evaluate the properties of thin-section casting relevant to turbocharger housings.

Technical Progress

Background

Current cast iron heavy diesel engine exhaust manifolds and turbocharger housings are being pushed beyond their temperature capabilities as normal duty cycles approach or exceed 750°C; the rapid and severe thermal cycling contributes to increased failures. The new cast CF8C-Plus austenitic stainless steel has now been commercialized, and business opportunities are being pursued and supported for this and other high-temperature applications. Caterpillar, Inc. and

ORNL have completed the systematic and thorough properties data base required by designers to optimize component design, and are currently characterizing the properties of trial or prototype commercially cast stainless steel components.

Approach

Multiple commercial heats of CF8C-Plus have been cast by several commercial foundries, including static sand and centrifugal casting methods. Now, both large and small prototype CF8C-Plus components have been cast. In July, 2004, a large turbine housing for an industrial gas-turbine was cast by MetalTek, International, Inc. from an 8000 lb heat of the new CF8C-Plus stainless steel. In 2005, three foundries obtained trial-licenses for CF8C-Plus steel, including MetalTek and Stainless Foundry & Engineering. By the end of 2005, over 31,000 lb of CF8C-Plus components have been cast, including exhaust manifolds, and some new, thin-walled piping. In 2005, new commercial heats of CF8C-Plus Cu/W were made, and in 2006 found to have more tensile strength and more creep resistance than CF8C-Plus at 750°C and above. In July 2006, Caterpillar chose CF8C-plus to use for the Caterpillar Regeneration System burner housing, which is now in production for exhaust components being included on all highway heavy-duty truck diesel engines in 2007.

Technical Progress – Caterpillar, Inc.

After completing prototyping and testing, Caterpillar is in production of the new cast CF8C-Plus stainless steel, which is being used for the housing of the Caterpillar Regeneration System (CRS) for on-highway truck diesel engines, beginning in 2007. The CRS device burns diesel fuel in the exhaust stream to heat the diesel particulate filter, in order to oxidize soot and regenerate the filter. This component is subject to extreme temperatures and thermal cycling, which makes the CF8C-Plus stainless steel a durable and relatively low-cost choice for this application.

This quarter, Caterpillar is in the final stages of licensing CF8C-Plus cast stainless steel for several different end-use applications, including turbocharger housings.

Technical Progress – ORNL

Stainless Foundry & Engineering (SF&E, one of the three current trial-licensees) completed casting, welding and testing of plates of CF8C-Plus steel for the ASTM Weld Procedure Qualification. CF8C-Plus was found to be weldable, consistent with several prior weld-trials, and the tensile and U-bend ductility data needed for ASTM Weld Procedure Qualification was obtained. Relative comparison of the new CF8C-Plus Cu/W showed it to also have similar good weldability, and similar good metal fluidity compared to the standard CF8C-Plus steel. SF&E (Ron Bird) is preparing the final package for approving a new alloy grade (HG10MNN) for the ASTM A297 Specification.

SF&E produced step castings of both CF8C-Plus and –Plus Cu/W to evaluate the properties of thin-section casting directly relevant to turbocharger housing components last quarter. 24 step-cast ingots were received at ORNL in December, 2006 for further evaluation, 12 of the standard CF8C-Plus steel and 12 of the new CF8C-Plus Cu/W steel. Tensile and some creep testing began this quarter and will be completed next quarter.

Communications/Visits/Travel

Detailed team communications between ORNL and Caterpillar occur regularly. The new 3-year CRADA began on July 21, 2002, when the previous CRADA ended and was scheduled to end on July 21, 2005. The two-year ORNL/Caterpillar CRADA extension was done last year until July 21, 2007.

Status of Milestones

Test properties of prototype components made of CF8C-Plus or –Plus Cu/W in support of diesel exhaust components, or other parts made by trial-licensee foundries for commercial applications (May, 2007). On-track for completion.

Publications/Presentations/Awards

Patents:

U.S. Patent 7,153,373 B2 on "Heat and Corrosion Resistant Cast CF8C Stainless Steel With Improved High Temperature Strength and Ductility," by P.J. Maziasz, T. McGreevy, M.J. Pollard, C.W. Siebenaler, and R.W. Swindeman, was obtained on December 26, 2006.

U.S. Patent Application 11/495,671 on "Heat and Corrosion Resistant Cast Austenitic Stainless Steel Alloy with Improved High Temperature Strength," by P.J. Maziasz, M.J. Pollard, and J.P. Shingledecker was filed on July 31, 2006.

Publications:

A draft paper "Developing New Cast Austenitic Stainless Steels with Improved High-Temperature Creep-Resistance" by P.J. Maziasz, J.P. Shingledecker, N.D. Evans and M.J.Pollard (PVP2007-26840) was submitted for publication in the Proceedings of CREEP8 – The Eighth International Conference on Creep and Fatigue at High Temperatures, to be held July 22-26, 2007 in San Antonio, TX.

Presentations:

"Designing New Steels for High Temperature Uses," by P.J. Maziasz was given as an invited ORICL Lecture for the Seminar Series IR-1 R&D100 Award Winning Research at ORNL, on Feb. 1, 2007 at Roane State Community College, Oak Ridge, TN.

"CF8C-Plus: A Material Developed by the 'Engineered Microstructure' Approach" by J.P. Shingledecker, was given as an Invited Seminar at the Department of Materials Science and Engineering at the University of Tennessee, Knoxville, TN on Mar. 20, 2007.

Development of Materials Analysis Tools for Studying SCR Catalysts

Thomas Watkins, Larry Allard, Doug Blom, Michael Lance, Harry Meyer and Larry Walker
Oak Ridge National Laboratory

Zheng Liu, Cheryl Klepser and Tom Yonushonis
Cummins Inc.

Objective

The purpose of this effort is to produce a quantitative understanding of the process/product interdependence leading to catalyst systems with improved final product quality, resulting in diesel emission levels that meet the 2010 emission requirements.

Samples and Approach

A Cummins catalyst supplier provided new commercial Fe-zeolite powder, both fresh and degreened, which are being examined with diagnostic tools developed under the CRADA. Here, degreened means the powder was heated to 500°C for 12 hours in air. Investigations of these candidate-production materials are being implemented on both the bench and engine research scale. These investigations include the examination of unused, reactor and engine-aged catalyst samples. Investigative tools included transmission electron microscopy (TEM), X-ray diffraction (XRD), X-ray photoelectron spectroscopy (XPS), Raman Spectroscopy and infrared spectroscopy (IR).

Introduction

Selective catalytic reduction (SCR) is one possible method to reduce NOx emissions. Here, a gaseous or liquid reductant is added to the exhaust gases and adsorbed on to the catalyst, sometimes a zeolite. The reductant reduces NOx to H_2O and N_2.[1] Urea is a typical reducing agent which can operate under lean or oxygen rich conditions as follows:[2]$(NH_2)_2CO + 2NO + 1/2O_2 \Rightarrow N_2 + 2H_2O + CO_2$.

A zeolite is classically defined as a crystalline, porous aluminosilicate. More recently, zeolites are defined as porous oxide structures with well-defined pore/channel structures and a high degree of crystallinity. There are an unlimited number of structures possible, making them particularly useful as molecular sieves.[3] There are many chemical interactions with zeolites which center around $Si\text{-}O_4$ and $(Al\text{-}O_4)^{-1}$ tetrahedra and the cations within the pores, supplying charge compensation. Zeolites are often used as ion exchangers in water softeners and shape selective catalysis. The cation with H+ becomes a strong acid, which is catalytically active.

Technical Highlight

Characterization of commercial Fe-zeolite powder, both fresh and degreened, in ORNL's aberration-corrected electron microscope (ACEM) was started during this quarter. High-angle annular dark-field imaging in scanning transmission mode (STEM) on the ACEM shows heavy elemental species in bright contrast relative to light element support material. A typical HA-ADF/bright-field pair of images that were acquired simultaneously is seen in Figure 1. The BF STEM image clearly shows the channels in the zeolite material, while the HA-ADF image shows

the Fe-rich phase in the specimen in bright contrast. The Fe-rich phase is distributed uniformly over the surface of the zeolite and ranges between 2-7 nm in spatial extent. The degreening process had a negligible effect on the distribution and size of the Fe-rich phase. This was also confirmed via XRD (see Figure 2). Further work on Fe/zeolite on monolith fresh and aged will be carried out in the coming quarter.

New X-Ray Photoelectron Spectrometer

ORNL has reached an agreement with Thermo Fisher Scientific to receive the first K-Alpha X-Ray Photoelectron Spectrometer (XPS) delivered to the U.S. for testing and evaluation (see Figure 3). This XPS instrument provides new capability for ORNL in detecting and measuring the surface composition of solid materials. In addition to providing elemental information, XPS goes further and helps to determine the chemical bonding state of surface-bound atoms. This kind of elemental and chemical information is foundational for understanding catalyst materials and catalytic mechanisms; determining corrosion products and their formation; and for monitoring thin film deposition and processes. The key characteristics of this instrument include: extreme surface sensitive chemical information (top 3-5 nm), good spatial resolution (30 micron), Ar+-ion depth profiling for determining composition as a function of depth and elemental and chemical mapping. This instrument will be applied to this CRADA.

References

1. Internet: en.wikipedia.org/wiki/Selective_catalytic_reduction.
2. I. Chorkendorff and J. W. Niemantsverdriet, Concepts of Modern Catalysis and Kinetics, Wiley-VCH Verlag GmbH & Co. KGaA, Weinheim, 2003, p. 400.
3. Internet: www.personal.utulsa.edu/~geoffrey-price/zeolite/zeo_narr.htm.

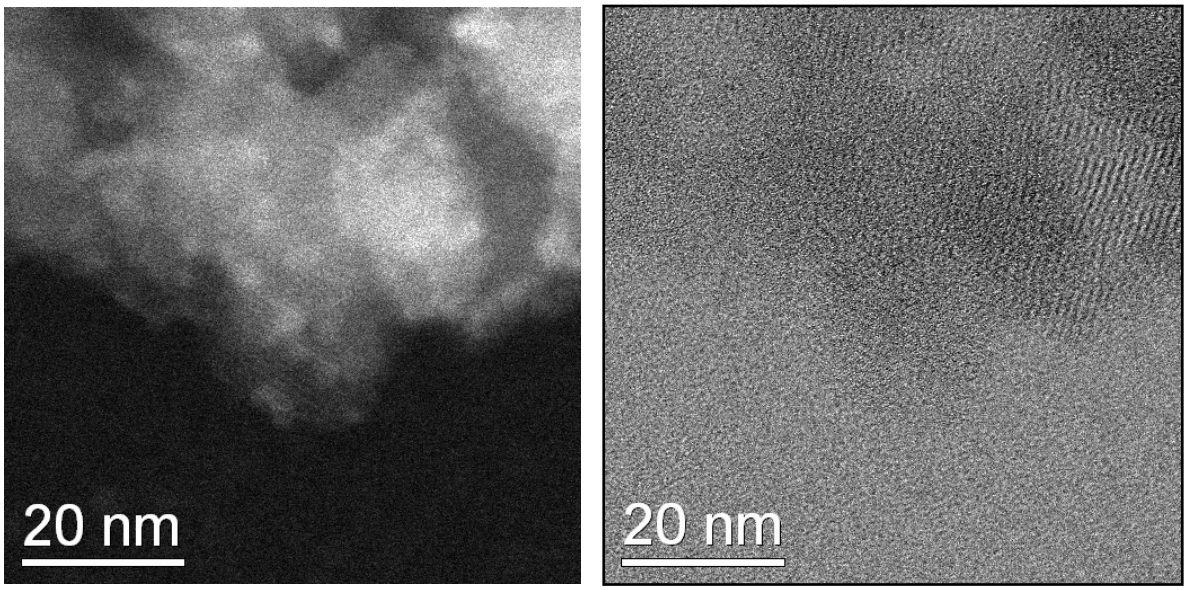

Figure 1. HA-ADF/BF pair of micrographs of fresh Fe/zeolite powder. The bright areas in the HA-ADF image are the Fe-rich phase.

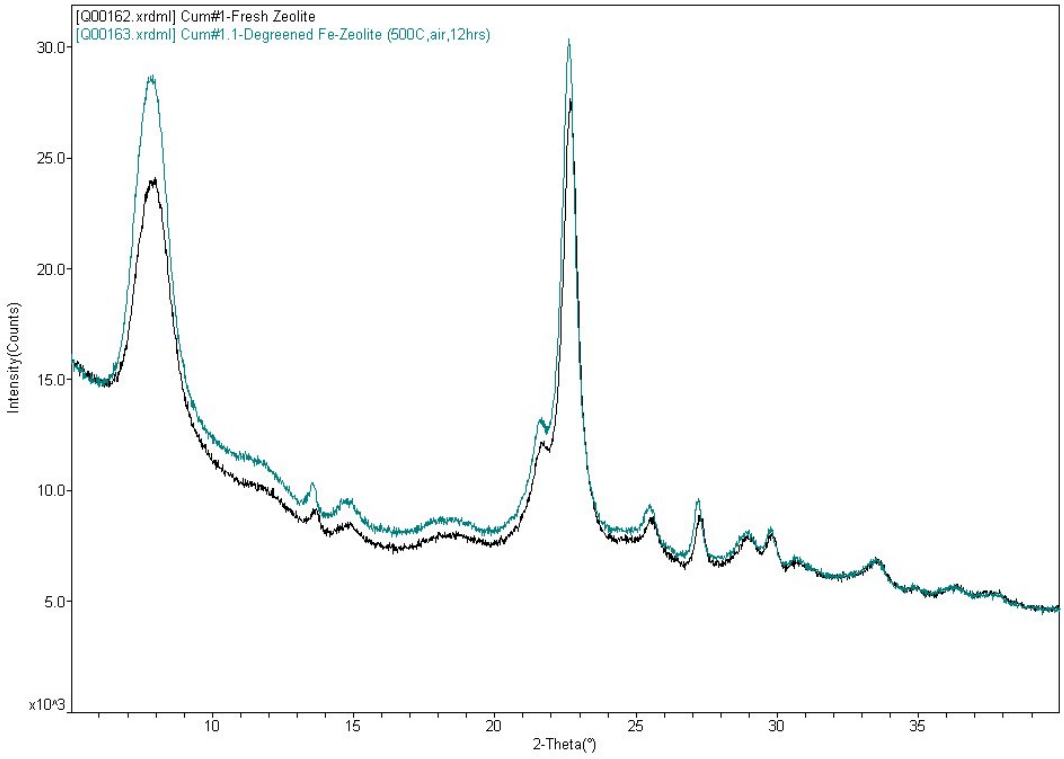

Figure 2 The x-ray pattern for the as-received and degreened Fe-zeolite powders.

Figure 3 - Thermo Fisher Scientific to receive the first K-Alpha X-Ray Photoelectron Spectrometer received by HTML.

Durability and Reliability of Ceramic Substrates for Diesel Particulate Filters

Amit Shyam and Thomas R. Watkins
Oak Ridge National Laboratory

Tom Yonushonis and Randy Stafford
Cummins Inc.

Objectives/Scope

To develop/implement test methods to characterize the physical and mechanical properties of ceramic diesel particulate filters (DPFs), and to implement a probabilistic-based analysis to quantify their durability and reliability.

Highlights

- The temperature dependence of the elastic modulus of porous cordierite substrates (for DPFs) was characterized up to 1000°C with resonant ultrasound spectroscopy (RUS).
- The orientation and loading rate dependence of the fracture characteristics of porous cordierite was investigated.

Technical Progress

The elastic modulus of the substrate is a key property for determining the mechanical reliability and thermal shock resistance of DPFs. The determination of the modulus poses a challenge due to the fragility of the substrates. Flat plates (40 x 20 x 0.375 mm) of porous cordierite were prepared by dry grinding methods reported earlier. Resonant ultrasound spectroscopy (RUS) was utilized to characterize the elastic modulus of this plate. The temperature dependence of the elastic modulus of the plate for three loading and unloading thermal cycles is reported in Figure 1. The temperature dependence of elastic modulus is unusual, in that the modulus values increase with temperature up to 1000°C. The initial room temperature elastic modulus value was calculated to be 11.85 GPa, which increased to 16.28 GPa at 1000°C. Thermal cycling decreases the modulus of the substrates and after three thermal cycles, the modulus of the same specimen decreased to 10.46 GPa. The increase in the modulus of the substrate with temperature is attributed to the closure of cracks at elevated temperature. Work is in progress to understand this unusual modulus increase with temperature. Additionally the elastic modulus of a honeycomb sample was also determined using RUS at ambient temperature. The sample possessed a 6 x 10 channel cross-section which was accounted for in the moment of inertia calculation. This sample was 16 x 27 x 84 mm and was found to have a Young's modulus of 14.2 GPa. More work in this area is planned.

The effect of orientation on the fracture toughness of porous cordierite, as determined by the double-torsion test method, is reported in Figure 2. Two extreme orientations are represented in this figure. The "parallel" orientation represents the specimen where the notch is parallel to the extrusion direction. In other words, the fracture toughness of this

specimen represents the crack propagation resistance of the material parallel to the honeycomb passages (Figure 2). The perpendicular orientation specimen K_{IC}, on the other hand represents the crack propagation resistance of the material in a direction that is perpendicular to the honeycomb passages. The perpendicular orientation has a fracture toughness of 0.45 $\pm$ 0.04 MPa√m, nearly 20% higher than the parallel orientation value. It is therefore, suggested that the ridges in the specimen provide a toughening mechanism. The fracture toughness of a DPF as determined by a ring crack with an arbitrary orientation would be in-between the two extreme values represented in Figure 2.

The effect of four orders of magnitude of loading-rate on the fracture toughness of porous cordierite at 20°C, 500°C and 800°C is reported in Figure 3. At all three temperatures, the fracture toughness increases with increasing loading rate suggesting an environmental influence on the fracture properties of the material under these conditions. It is to be noted that the term fracture toughness has been used in this context as an environmentally modified fracture toughness. The results reported in Figure 3 are consistent with the slow crack growth resistance of this material which has already been characterized.

Milestones

Quantify the growth rate of radial cracks in DPFs subjected to arbitrary loading schedule. (March 2007). (Completed)

Meetings

Bimonthly meetings with Cummins personnel were held during the reporting period.

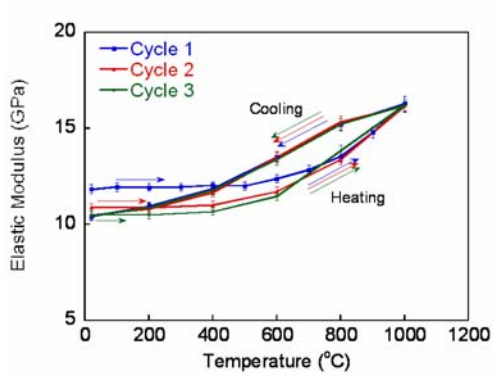

Figure 1. The temperature dependence of the elastic modulus of porous cordierite. The test specimen was subjected to three thermal loading cycles with a maximum temperature of 1000°C.

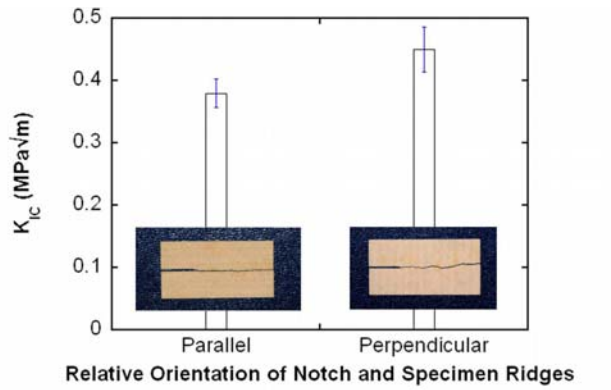

Figure 2. The effect of notch orientation on the fracture toughness of porous cordierite, as determined by the double-torsion method.

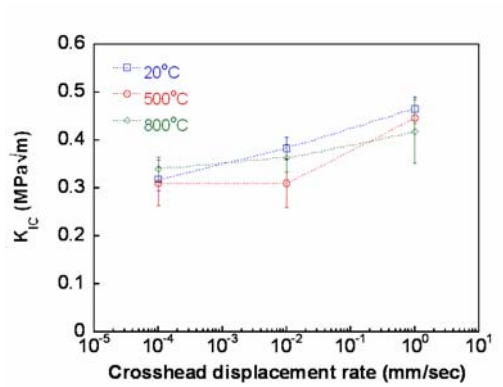

Figure 3. The effect of loading-rate on the fracture toughness of porous cordierite. The fracture toughness value increases with increasing loading-rate.

Catalysis by First Principles - Can Theoretical Modeling and Experiments Play a Complimentary Role in Catalysis?

C. Narula, W. Shelton, M. Moses, L. Allard
Oak Ridge National Laboratory

Objective/Scope

This research focuses on an integrated approach between computational modeling and experimental development, design and testing of new catalyst materials, that we believe will rapidly identify the key physiochemical parameters necessary for improving the catalytic efficiency of these materials. The results will have direct impact on the optimal design, performance, and durability of supported catalysts employed in emission treatment e.g. lean NO_x catalyst, three-way catalysts, oxidation catalysts, and lean NO_x traps etc.

The typical solid catalyst consists of nano-particles on porous supports. The development of new catalytic materials is still dominated by trial and error methods, even though the experimental and theoretical bases for their characterization have improved dramatically in recent years. Although it has been successful, the empirical development of catalytic materials is time consuming and expensive and brings no guarantees of success. Part of the difficulty is that most catalytic materials are highly non-uniform and complex, and most characterization methods provide only average structural data. Now, with improved capabilities for synthesis of nearly uniform catalysts, which offer the prospects of high selectivity as well as susceptibility to incisive characterization combined with state-of-the science characterization methods, including those that allow imaging of individual catalytic sites, we have compelling opportunity to markedly accelerate the advancement of the science and technology of catalysis.

Computational approaches, on the other hand, have been limited to examining processes and phenomena using models that had been much simplified in comparison to real materials. This limitation was mainly a consequence of limitations in computer hardware and in the development of sophisticated algorithms that are computationally efficient. In particular, experimental catalysis has not benefited from the recent advances in high performance computing that enables more realistic simulations (empirical and first-principles) of large ensemble atoms including the local environment of a catalyst site in heterogeneous catalysis. These types of simulations, when combined with incisive microscopic and spectroscopic characterization of catalysts, can lead to a much deeper understanding of the reaction chemistry that is difficult to decipher from experimental work alone.

Thus, a protocol to systematically find the optimum catalyst can be developed that combines the power of theory and experiment for atomistic design of catalytically active sites and can translate the fundamental insights gained directly to a complete catalyst system that can be technically deployed.

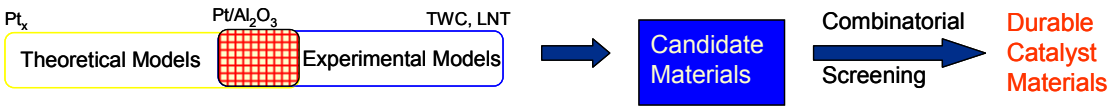

Although it is beyond doubt computationally challenging, the study of surface, nanometer-sized, metal clusters may be accomplished by merging state-of-the-art, density-functional-based, electronic-structure techniques and molecular-dynamic techniques. These techniques provide accurate energetics, force, and electronic information. Theoretical work must be based electronic-structure methods, as opposed to more empirical-based techniques, so as to provide realistic energetics and direct electronic information.

A computationally complex system, in principle, will be a model of a simple catalyst that can be synthesized and evaluated in the laboratory. It is important to point out that such a system for experimentalist will be an idealized simple model catalyst system that will probably model a "real-world" catalyst. Thus it is conceivable that "computationally complex but experimentally simple" system can be examined by both theoretical models and experimental work to forecast improvements in catalyst systems.

Our Goals are as follows:

- Our theoretical goal is to carry out the calculation and simulation of realistic Pt nanoparticle systems (i.e., those equivalent to experiment), in particular by addressing the issues of complex cluster geometries on local bonding effects that determine reactivity. As such, we expect in combination with experiment to identify relevant clusters, and to determine the electronic properties of these clusters.
- Our experimental goal is to synthesize metal carbonyl clusters, decarbonylated metal clusters, sub-nanometer metal particles, and metallic particles (~5 nm) on alumina (commercial high surface area, sol-gel processed, and mesoporous molecular sieve), characterize them employing modern techniques including Aberration Corrected Electron Microscope (ACEM), and evaluate their CO, NO_x, and HC oxidation activity.
- This approach will allow us to identify the catalyst sites that are responsible for CO, NOx, and HC oxidation. We will then address support-cluster interaction and design of new durable catalysts systems that can withstand the prolonged operations.

<u>Technical Highlights</u>

Our results on experimental studies of Platinum-Alumina Systems are summarized in the following paragraphs. The results demonstrate the impact of substrate morphology and structure (γ- vs. θ-Al_2O_3) on the catalytic behavior.

Experimental Studies:

We reported last quarter that atomic resolution imaging of 1 nm Pt/γ-Al_2O_3 by the ACEM showed the presence of single atoms and 2-3 atom clusters in addition to several 10-20 atom clusters of Pt. Our theoretical studies suggested that small atomic Pt clusters on inert supports behave similarly to free Pt clusters.

These results are in contrast to reported structure for Pt/γ-alumina. The Z-contrast imaging reports in literature describe the presence of 3-atom clusters and allocate anomalous long Pt-Pt bonds to OH terminated Pt clusters. Recent EXAFS studies, on the other hand, suggest thermal metal-metal bond contraction after hydrogen reduction of Pt/γ-Al_2O_3 whose TEM shows particles in 0.5-1.5 nm range centered at ~0.9 nm consisting of 15±9 atoms on average.

In order to study the impact of substrate morphology, we synthesized 2%Pt/θ-Al_2O_3. Since the structure of θ-Al_2O_3 is simpler than γ-Al_2O_3, it is possible to theoretically model reaction chemistry by density functional theory on the catalyst sites in 2%Pt/θ-Al_2O_3. The complexity of structure for γ-Al_2O_3, on the other hand, is quite taxing on computing resources.

2%Pt/ θ -Al_2O_3 Catalyst: Impact of Substrate

Discerning the impact of substrate in Pt-γ-Al_2O_3 system is difficult due to its structural complexity. The θ-Al_2O_3, on the other hand, has a well ordered crystal lattice. Thus, any difference in the catalytic activity of Pt-θ-Al_2O_3 as compared with Pt-γ-Al_2O_3 can be allocated to substrate morphology change and resulting impact on the catalyst. This led us to investigate 1nm 2%Pt/θ-Al_2O_3 catalyst under CO oxidation conditions and monitor the structural changes by STEM. As observed in the Pt-γ-Al_2O_3, the exposure of 1nm 2%Pt/θ-Al_2O_3 to CO oxidation initiation conditions resulted in changes to the Pt nano-structure.

a. STEM images of fresh 2%Pt/θ,sol-Al_2O_3 [Figure 1] catalyst show the average Pt size to be 0.9 nm and to range from 0.6-1.3 nm. The particle size distribution is virtually identical to that seen for Pt supported on γ-Al_2O_3 [Table 1].

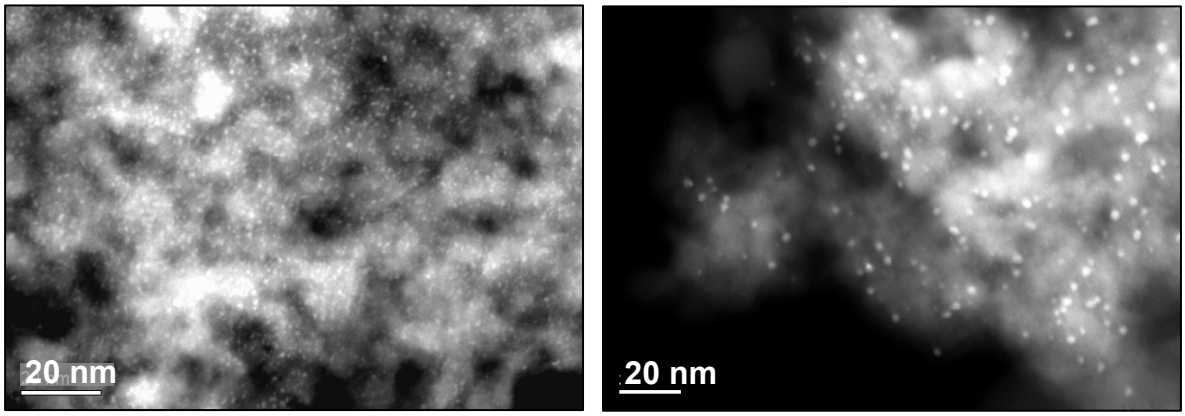

Figure 1. STEM images of fresh 1nm 2%Pt/θ-alumina (left) and after CO oxidation initiation testing (right). Both images show 20 nm scale bars.

Table 1. Average Pt particle size and ranges seen by STEM before and after CO oxidation testing.

	Fresh	**Initiation**	**Full Range 3x**
1nm Pt/γ-alumina	0. 9 nm (0.6-1.4 nm)	1.9 nm (0.7-3.8 nm)	2.0 nm (0.7-5.6 nm)
25nm Pt/γ-alumina	12.9 nm (3.4-36.7 nm)	13.1 nm (1.4-87.9 nm)	17.0 nm (1.7-68.7 nm)
1nm Pt/θ,sol-alumina	0.9 nm (0.6-1.3 nm)	1.8 nm (0.6-4.0 nm)	2.0 nm (0.7-5.1 nm)
25nm Pt/θ,sol-alumina			

b. The CO oxidation reaction initiates around 170-180ºC with ~5% conversion. Analysis of the catalyst which was removed from the CO oxidation conditions immediately after

initiation began was loaded on a TEM sample grid by dry-dipping. STEM imaging indicates an average Pt size of 1.8 nm with the clusters/particles ranging in size from 0.6-4.0 nm, see Figure 1. Figure 2 compares the particle size distribution of the initiation used catalyst with that seen for the fresh catalyst.

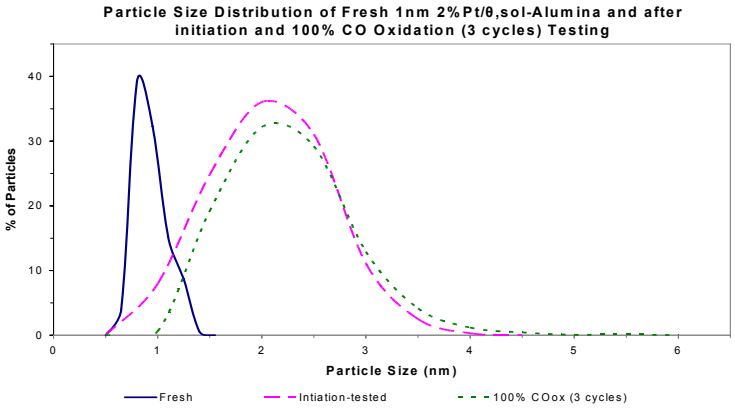

Figure 2. Particle size distribution comparison of 1nm 2%Pt/θ-alumina catalyst by STEM imaging of multiple areas, for fresh and CO oxidations tested samples (initiation and 100% three cycles of COox). Sizes have been sorted into ranges for this graph and all begin and end at 0%.

c. The effect of quantitative conversion on Pt sintering of the (1 nm) 2%Pt/θ-Al_2O_3 catalyst was also evaluated using STEM imaging. The reaction temperature was increased gradually to attain quantitative CO oxidation, the reaction was stopped, and the reactor was cooled under inert conditions. The reaction was restarted and allowed to attain quantitative CO oxidation. After a third cycle, the catalyst sample was collected. STEM imaging of multiple areas indicates an average Pt size of 2.0 nm that ranges from 0.7-5.1 nm [Figure 3]. Figure 2 shows that after 3 cycles of quantitative conversion the particle size distribution is similar to that seen after exposure to only initiation conditions, except that it tails out to a slightly higher size range.

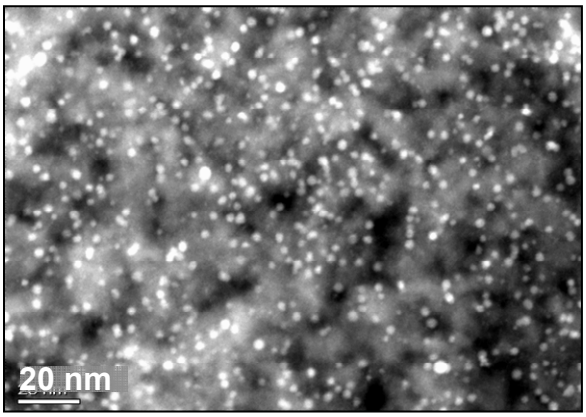

Figure 3: STEM images of 1nm 2%Pt/γ-Al_2O_3 after three cycles of quantitative CO oxidation.

While a change in nano-structure was seen between the fresh 2%Pt/θ-Al_2O_3 catalyst and after it had been exposed to CO oxidation initiation conditions, little change was observed between exposure to initiation and 3 cycles of quantitative oxidation. This nano-structural observation is virtually identical to what we observed for the same catalyst supported on γ-Al_2O_3, see Table 1 and Figure 4. The two different supported catalysts' only apparent difference is in the energy (temperature) need to reach these stages [Figure 5]. The θ-Al_2O_3 support approaches

quantitative conversion around 200-210°C while the γ-Al_2O_3 supported catalyst doesn't until the temperature is over 300ºC. The θ-Al_2O_3 catalyst with 1nm Pt is more comparable to the pre-sintered γ-Al_2O_3 catalyst which has Pt particles around 12 nm. However, even the 12nm 2%Pt/γ-Al_2O_3 catalyst requires higher temperatures (240-250ºC) to approach quantitative conversion.

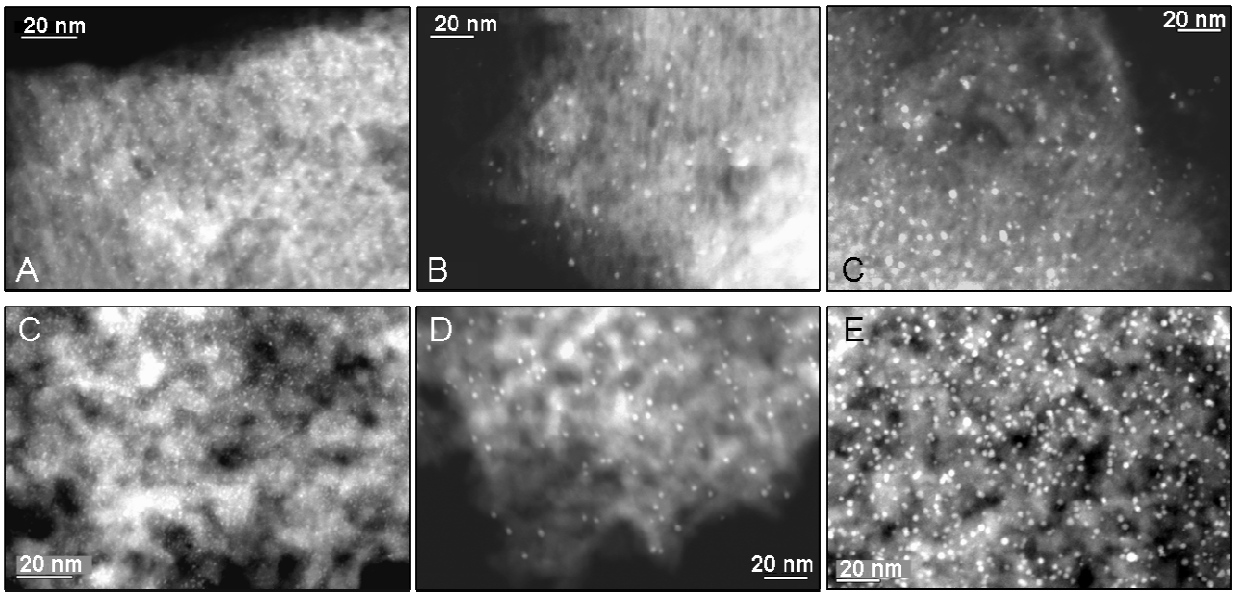

Figure 3. STEM images of 2%Pt/γ-Al_2O_3 (top row) and 2%Pt/θ-Al_2O_3 (bottom row) as fresh catalyst (A, C), after CO oxidation initiation (B, D) and after 3 cycles of quantitative CO oxidation (C, E)

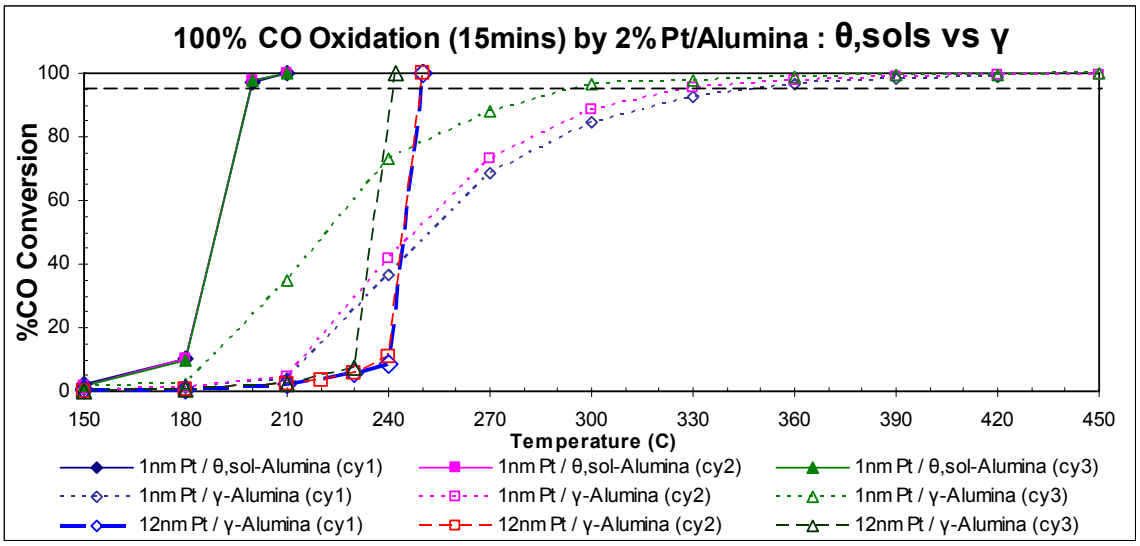

Figure 4. Quantitative CO oxidation cycled 3 times presented as a function of temperature comparing the different temperature ramps required for 1 nm Pt on θ-Al_2O_3, 1nm Pt on γ-Al_2O_3 and 12 nm Pt on γ-Al_2O_3. The horizontal dashed line indicates 90% oxidation as the catalyst approach quantitative CO conversion.

These results are interesting and we are carrying out further studies to understand the substrate morphology impact on catalyst reactivity.

Next Steps: We plan to carry out the following tasks:

- We plan to complete CO oxidation studies of already synthesized Pt clusters (1 nm and pre-sintered 2%Pt/θ-Al_2O_3) and MgO to determine the metal species involved in CO oxidation. The results will be compared with the results from theoretical calculation. If consistent, we will proceed with the evaluation of the catalysts for NO_x and hydrocarbon oxidation.

- We will synthesize Pt clusters on sol-gel and molecular sieve alumina. This will create a matrix of samples with varying Pt particles size and oxidation on alumina substrates with increasing surface area and pore structure. We will carry out CO, NO_x and HC oxidation on these samples to study the effect of morphological changes in substrates leading to changes in metal substrate interactions.

- We will continue to investigate the thermochemistry of CO and NO oxidation on free Pt and Pt oxide clusters as well as the properties of Pt and Pt oxide clusters supported on metal oxides (include magnesia and alumina). These investigations will help us gain a better understanding of the structural and catalytic properties of the supported Pt clusters and identify the effect of the support on these important properties.

Publications/Presentations

1. Narula, C. K., Moses, M.J., Xu, Y., Blom, D.A., Allard, L.F., Shelton, W.A. "Catalysis by Design – Theoretical and Experimental Studies of Model Catalysts." *SAE no. 2007-01-1018*, 2007.
2. Narula, C. K., Moses, M.J., Allard, L.F. "Analysis of Microstructural Changes In Lean NO_x Trap Materials Isolates Parameters Responsible for Activity Deterioration" *SAE no. 2006-01-3420*, 2006.
3. Narula, C.K., Moses, M.J. (speaker), Allard, L.F. "Analysis of Microstructural Changes in Lean NO_x Trap Materials Isolates Parameters Responsible for Activity Deterioration." Society of Automotive Engineers Powertrain and Fluid Systems Conference, Toronto, Canada, October 2006.
4. Narula, C. K. (speaker), Moses, M.J., Allard, L.F. "Analysis of Microstructural Changes in Lean NO_x Trap Materials Isolates Parameters Responsible for Activity Deterioration." SAE 2007 World Congress, Detroit, MI, April 2007. (abstract accepted)
5. Narula, C. K., Moses, M.J., Blom, D.A., Allard, L.F. "Nano-Structural Changes in Supported Pt Catalysts during CO Oxidation." North American Catalysis Society Meeting, Houston, TX, June 2007. (abstract accepted)

Ultra-High Resolution Electron Microscopy for Characterization of Catalyst Microstructures and De-activation Mechanisms

L. F. Allard, D. A. Blom, C. K. Narula, M. A. O'Keefe, M. J. Yacaman, and S. A. Bradley
Oak Ridge National Laboratory

Objective/Scope

The objective of the research is to characterize the microstructures of catalyst materials of interest for the treatment of NO_x emissions in diesel and lean-burn gasoline engine exhaust systems. The research heavily utilizes new capabilities and techniques for ultra-high resolution transmission electron microscopy with the HTML's aberration-corrected electron microscope. The research is focused on understanding the effects of reaction conditions on the changes in morphology of heavy metal species on "real" catalyst support materials (typically oxides), and the understanding of the structures of model mono-, bi- and multi-metallic catalyst systems of known particle composition. With the former systems, these changes are being studied utilizing samples treated in both steady-state bench reactors and a special *ex-situ* catalyst reactor system especially constructed to allow appropriate control of the reaction. Model samples of nanoparticulates of controlled composition on carbon or oxide supports are also being studied in collaboration with the catalysis group at the University of Texas-Austin (Prof. M. Jose-Yacaman and students). Studies of the behavior of Pt species on oxide substrates are also being conducted with colleague S. A. Bradley of UOP Co.

Technical Progress

The arrangement of heavy metal species in "as-prepared" catalysts on common supports is not well understood, notwithstanding decades of study on the preparation and properties of such catalysts. Aging or calcining treatments often cause atomic dispersions of heavy metals species to coarsen into discrete particles of size >2 nm, with crystal lattices that can be imaged using conventional high-resolution bright-field imaging techniques. High-angle annular dark-field (HA-ADF), or Z-contrast, imaging in an aberration-corrected scanning transmission electron microscope (STEM) is the best direct technique for studying monoatomic and multi-atom "rafts" of heavy metals which form prior to growth into discrete nanoparticles. The present study illustrates the advanced capability of imaging at the sub-Ångström level to characterize catalysts, via the example of Pt dispersed on γ-Al_2O_3. Catalysts were prepared by impregnating the support materials with 0.35 wt. % Pt, and oxidizing the material at 525ºC. The resulting oxidized catalyst was imaged in ORNL's JEOL 2200FS FEG STEM/TEM, which is outfitted with a hexapole aberration-corrector (CEOS GmbH, Heidelberg, Germany) on the probe forming optics. *Ex-situ* exposure of the catalyst to 4%H_2 in Ar for 15 minutes at 300°C was followed by re-examination in the microscope, followed by a subsequent series at 350°C for 15 minutes. The nominal probe diameter for STEM imaging is 0.07 nm at an illumination acceptance semi-angle of 26.5 mrad. For this aperture size, the probe-forming optics are not limited by the geometrical aberrations of the final lens but instead are limited by the information limit of the microscope and local environment [1]. The goal of the investigation was to determine the evolution of the Pt dispersion from the oxidized condition to the activated reduced condition.

For the oxidized Pt on γ-Al_2O_3 catalyst, individual Pt atoms were observed randomly decorating the catalyst support. Detailed examination revealed that these were mainly individual Pt atoms or small clusters of Pt atoms (Fig. 1). The atoms moved over small distances during the observation, but were not in general highly mobile on the surface. Following reduction at 300°C, the number of small clusters had increased, while the prevalence of single Pt atoms

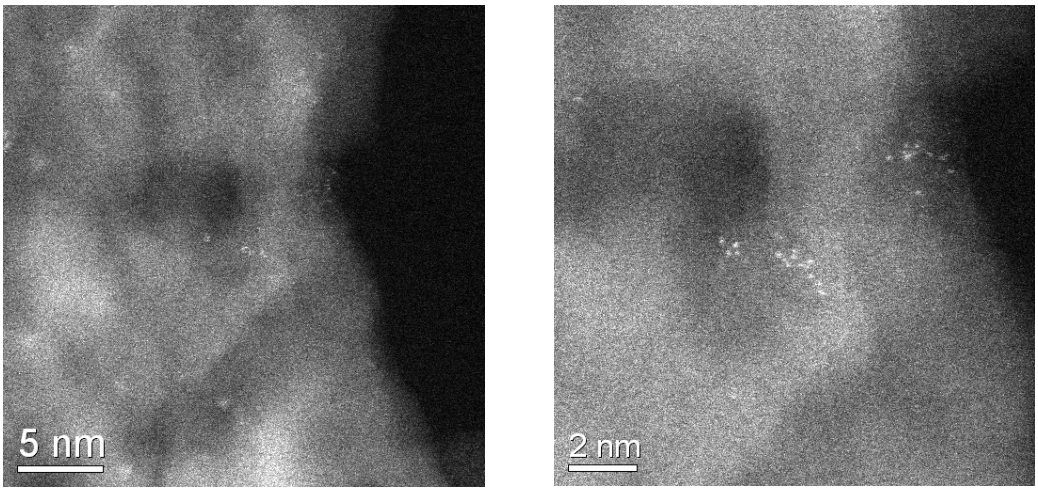

Fig. 1. Individual Pt atoms and small clusters decorating γ-Al_2O_3 support in the oxidized condition.

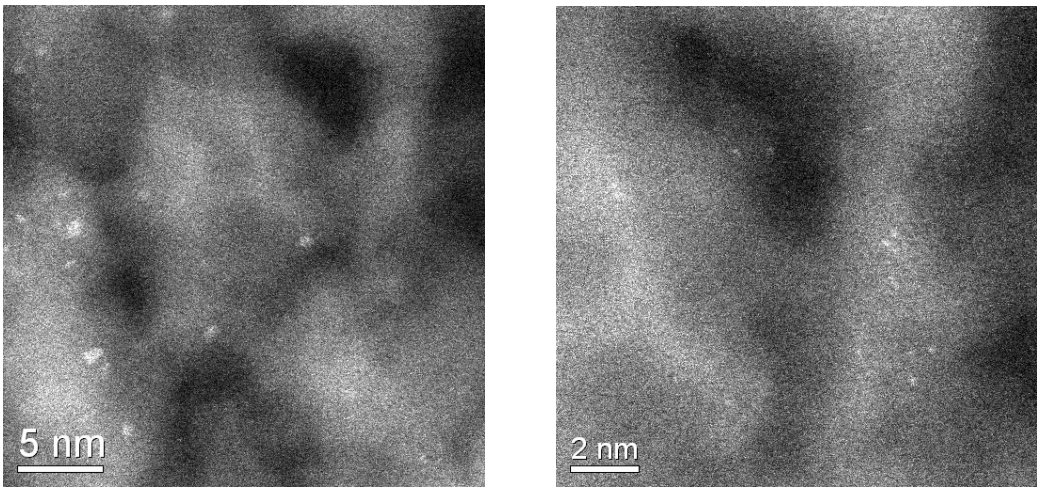

Fig. 2. Pt atoms and clusters on γ-Al_2O_3.after reduction at 300°C. Additional clusters are evident as compared to the oxidized case. Small tilt of the alumina support has occurred.

had decreased (Fig. 2). In addition, the alumina support was observed to have a tendency to move slightly relative to the holey carbon support film or to rotate slightly during the *ex situ* exposure. Additional reduction at 350°C only slightly changed the structure of the Pt metal species, primarily in the number of atoms in the typical cluster (Fig. 3).

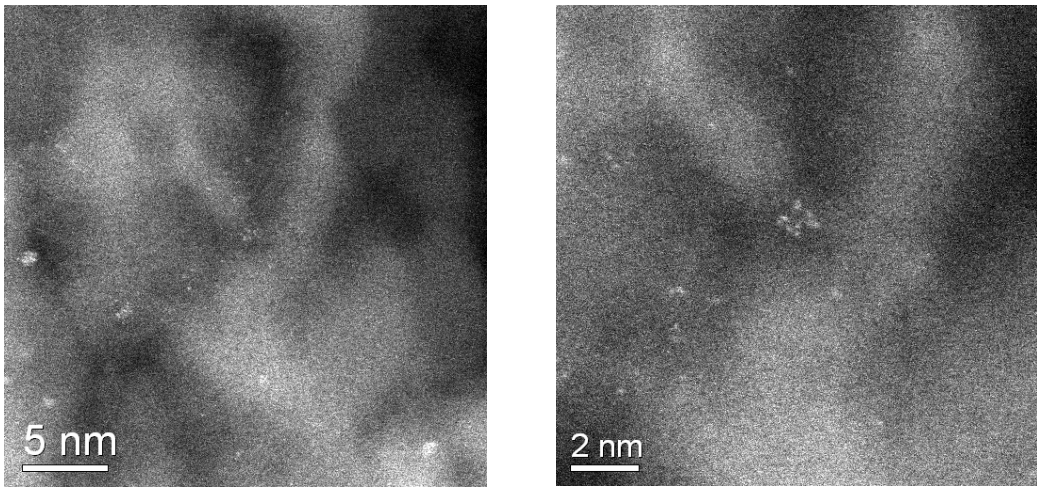

Fig. 3. After 350°C reduction, single atoms are still seen, and the size of the clusters has increased.

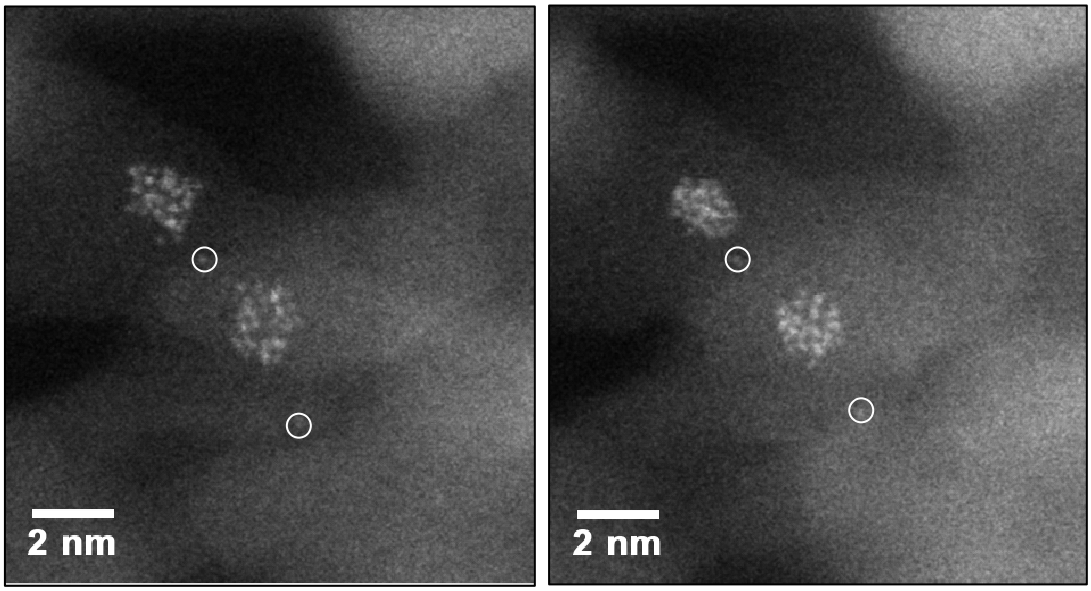

Fig. 4. Two frames from a "movie" sequence compiled from several (~10) images of the same sample area, showing size of Pt clusters seen after 700°C reductions, and the behavior under the influence of the electron beam.

Additional reduction experiments were conducted up to 700°C, with the observation that cluster size continued to gradually increase. Figure 4 shows 2 images of the same area of the catalyst after reduction again for 15 minutes. The Pt species have aggregated into "rafts" 1.5-20 nm in size, which, under the influence of the electron beam, tend to re-arrange atomically, but are relatively stable in position relative to the alumina support. Interestingly, as has been shown before, single atoms often tend to be "pinned" to the support, and do not always join a raft. Such atoms are likely not to provide active sites for catalysis. These experiments, utilizing the ultimate imaging capabilities of the ACEM to show the behavior of catalyst atoms on oxide supports with processing, are providing baseline information to further understand mechanism of catalytic reactions.

References

[1] D. A. Blom, L. F. Allard, S. Mishina, and M. A. O'Keefe, *Microsc. and Microanal.* **12,** 483, 2006.

Status of Milestones

On schedule

Communications/Visits/Travel

March 2007. L. F. Allard presented the keynote address at the University of Texas, Austin Department of Chemical Engineering Workshop on Aberration-Corrected Electron Microscopy. The talk was entitled: "Looking at Atoms with the Aberration-Corrected Electron Microscope: The World Through "Rose-Colored" Lenses."

Publications

"Studies of Pt Cluster Evolution During Reduction;" D. A. Blom, S. A. Bradley, W. Sinkler and L. F. Allard, submitted to Microscopy Society of America, 2007.

Life Prediction of Diesel Engine Components

H. T. Lin, T. P. Kirkland, and A. A. Wereszczak
Oak Ridge National Laboratory

Nate Phillips and Nan Yang
Caterpillar Inc.

Objective/Scope

The valid prediction of mechanical reliability and service life is a prerequisite for the successful implementation of structural ceramics and advanced intermetallic alloys as internal combustion engine components. There are three primary goals of this research project which contribute toward that implementation: the generation of mechanical engineering data from ambient to high temperatures of candidate structural ceramics and intermetallic alloys; the microstructural characterization of failure phenomena in these ceramics and alloys and components fabricated from them; and the application and verification of probabilistic life prediction methods using diesel engine components as test cases. For all three stages, results are provided to both the material suppliers and component end-users.

The systematic study of candidate structural ceramics (primarily silicon nitride) for internal combustion engine components is undertaken as a function of temperature (< 1200°C), environment, time, and machining conditions. Properties such as strength and fatigue will be characterized via flexure and rotary bend testing.

The second goal of the program is to characterize the evolution and role of damage mechanisms, and changes in microstructure linked to the ceramic's mechanical performance, at representative engine component service conditions. These will be examined using several analytical techniques including optical and scanning electron microscopy. Specifically, several microstructural aspects of failure will be characterized:

(1) strength-limiting flaw-type identification;
(2) edge, surface, and volume effects on strength and fatigue size-scaling;
(3) changes in failure mechanism as a function of temperature;
(4) the nature of slow crack growth; and
(5) what role residual stresses may have in these processes.

Lastly, numerical probabilistic models (i.e., life prediction codes) will be used in conjunction with the generated strength and fatigue data to predict the failure probability and reliability of complex-shaped components subjected to mechanical loading, such as a silicon nitride diesel engine valve. The predicted results will then be compared to actual component performance measured experimentally or from field service data. As a consequence of these efforts, the data generated in this program will not only provide a critically needed base for component utilization in internal combustion engines, but will also facilitate the maturation of candidate ceramic materials and a design algorithm for ceramic components subjected to mechanical loading in general.

Technical Highlights

Silicon nitride and TiAl exhaust valves

During this reporting period the stems of some selected 500-h-tested valves of both silicon nitride and TiAl were machined for retained strength characterization after NDE evaluation at ANL. The objective of this destructive study was to evaluate the effect of the surface roughness, which was introduced due to the high-speed reciprocal contacts between valve and valve guide during 50-h engine test, on the mechanical reliability and performance of materials. The half-cylindrical flexure bars were machined from the valve stem section and tested using the four-point flexure approach. The inner and outer spans of the flexure fixture were 30 and 60 mm, respectively. Note that similar specimens machined from as-received valves would be tested for comparison. Figure 1 compares the fracture strengths between 500-h tested and as-received valves. Results show that as for the silicon nitride valves the 500-h-tested valves exhibit strength values that are about 10% higher than those in as-received condition. Similarly, the 500-h tested TiAl valves exhibited about 11-19% higher strength than those as-received ones as well. These higher strength values of valve stem section measured are consistent with the surface roughness measurements reported previously that there was a decreased in Ra values (roughness) due to the reciprocal polishing effect. On the other hand, initial analysis of optical fractography for all of the fractured valves showed that the failure initiated at the surface region (Fig. 2). Detailed SEM analysis will be carried out on selected pieces to elucidate the cause of failure.

High-temperature Creep of TiAl intermetallic alloys

Studies of long-term creep behavior in air of TiAl alloys manufactured by Daido and Howmet were continued during this reporting period. Two types of TiAl cylindrical creep specimens different in final densification process (i.e., one is HIP and the other one is Non-HIP) manufactured by Daido, Tokyo, Japan, and designated as RNT650 were received from end user. Also, TiAl tensile specimens manufactured by Howmet, Michigan, USA, and designated as 45XD were also received for evaluation. The test conditions specified are relevant to the temperature and tensile stress profiles encountered by TiAl turbo wheel under the application conditions based on the FEA modeling. The database generated will then be used for verification of probabilistic life prediction of turbo wheel under engine operation conditions by the end users, and could also provide important feedbacks to material suppliers for process modification to further improve its high-temperature mechanical performances. During this reporting period creep tests were focused on the creep response of Daido non-HIP and Howmet TiAl alloy. Note that tensile creep results of Daido TiAl alloy reported previously indicated that there was a minor effect of processing (HIP vs. non-HIP) under the similar test conditions employed at temperature < 700°C. The preliminary creep strain versus time curves showed that the Daido non-HIP RNT650 exhibited a long transient stage (~500 h) prior to the transition into the steady state, which was in sharp contrast to the Howmet 45XD that exhibited a relative short transient stage (<100 h), as shown in Figs. 3 and 4. Also, the Howmet 45XD exhibited lower creep resistance as compared to Daido RNT650 under the similar test conditions. The apparent difference in transient stage as well as creep resistance could arise from the difference in microstructure (grain size and lamellar thickness). Microstructure analysis showed that Daido RNT650 had a ~400 µm grain (colony) size and Howmet 45XD had a smaller grain size of 100 µm. Nonetheless, more creep tests under various test temperatures and applied stress levels

would be carried out to understand the effect of microstructure on the creep response and also the creep controlling mechanism as a function of temperature and stress level for both alloys.

Status of Milestones

Milestone: "Complete mechanical testing and analysis of prototype silicon nitride and TiAl valves after natural gas engine field test." On schedule.

Communications / Visitors / Travel

Communication with Nate Phillips at Caterpillar, and Norberto Domingo and Michael Kass at NTRC on the updated status of the preparation works for the next phase 500-h engine test for Si_3N_4 and TiAl exhaust valves.

Communication with Nate Phillips at Caterpillar on the mechanical testing on the Ceradyne SN147 silicon nitride cylindrical rods after machined via various machining parameters.

Communications with Nan Yang at Caterpillar on the update of tensile creep tests for both Daido and Howmet TiAl materials.

Problems Encountered

There was a major problem with the charge amplifier and it had to be repaired by the manufacturer, which would cause some delay in the initiation of next 500-h engine test schedule.

Publications

None

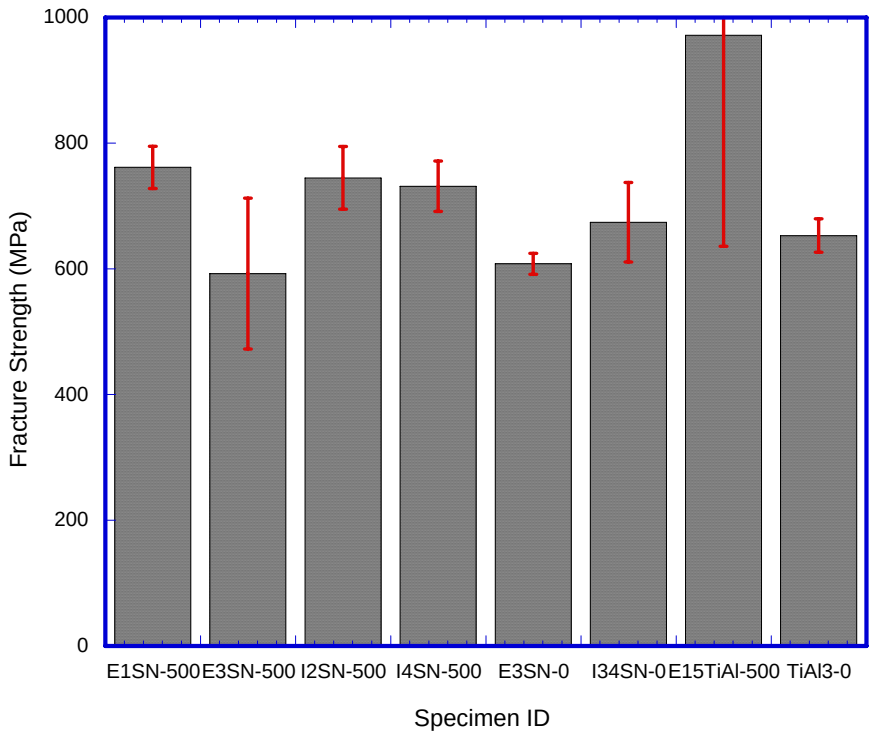

Figure 1. Fracture strength of half-cylindrical flexure specimens of silicon nitride and TiAl after 500-h engine test and in as-received condition.

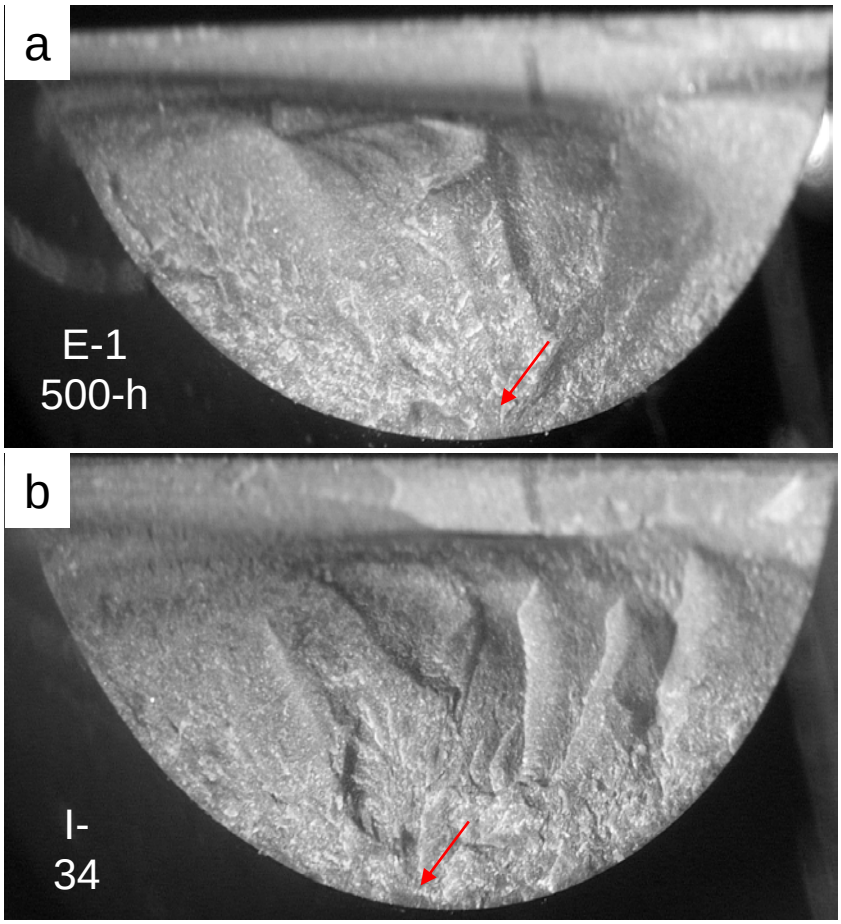

Figure 2. Optical fractography of half cylindrical SN235P silicon nitride exhaust valves after 500-h test (a) and in as-received condition (b).

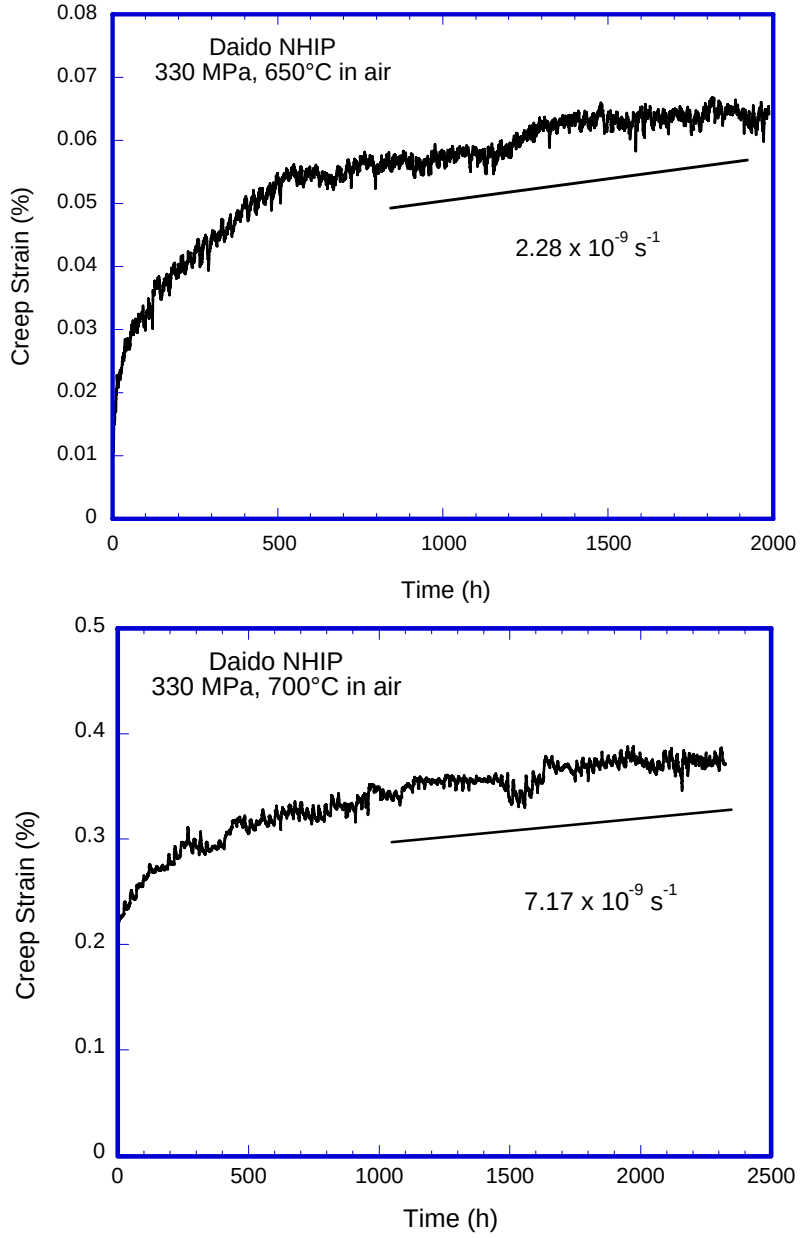

Figure 3. Creep train versus time curve of Daido RNT650 TiAl with non-HIP condition.

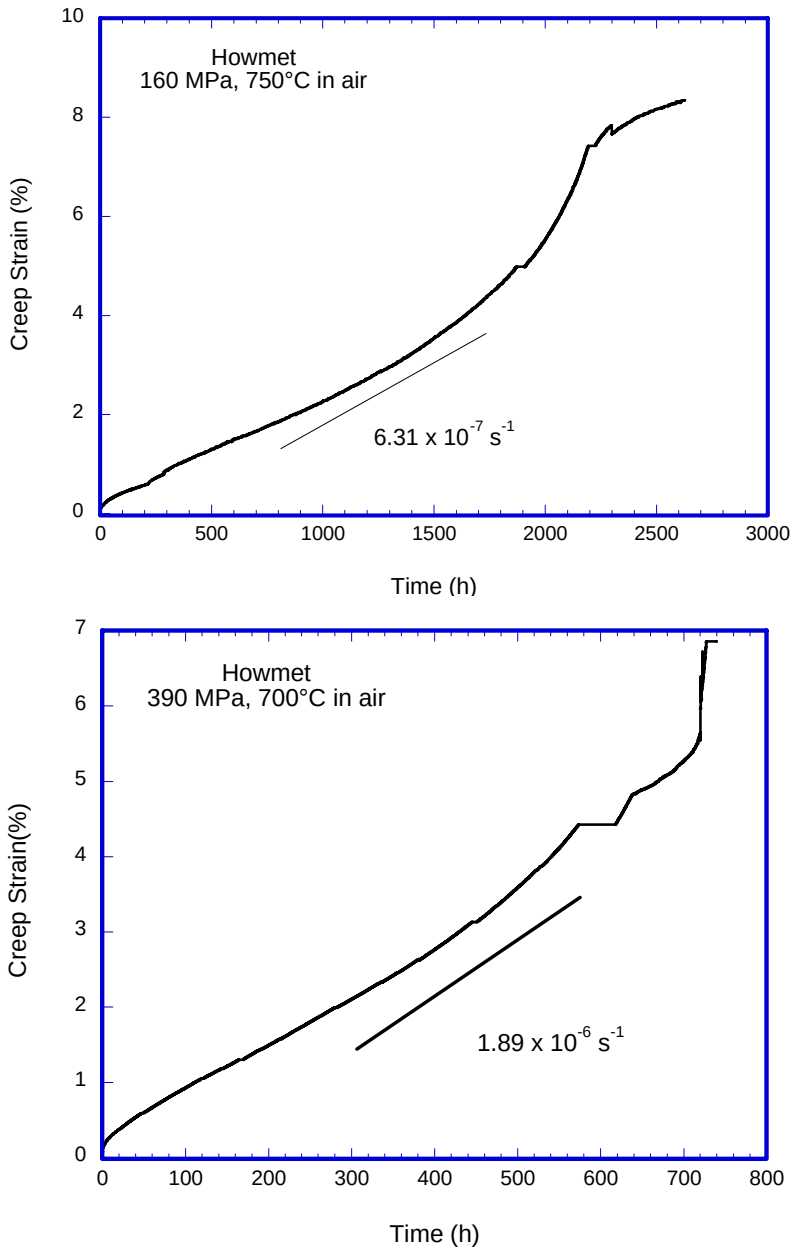

Figure 4. Creep train versus time curve of Howmet 45XD TiAl.

Powder Processing of Nanostructured Alloys Produced by Machining

S. Chandrasekar, K. P. Trumble, and W. D. Compton
Purdue University

Objective/Scope

Work has continued on production of bulk ultrafine-grained (UFG) alloys by machining, and development of methods for consolidation of UFG particulate created by machining. This report describes recent work on manufacture of bulk forms by large-strain extrusion machining (LSEM).

Technical Highlights

Figure 1 illustrates a plane strain LSEM process wherein material (chip) of controlled thickness and an UFG microstructure is produced by machining and extrusion imposed in a single step using a specially designed tool. In this configuration, an LSEM tool moves into a disk-shaped workpiece rotating at a constant peripheral speed, V. The tool consists of two components – a bottom section with a sharp cutting edge inclined at a rake angle (α) (Figure 1); and a wedge-shaped top section that acts as a constraining edge. Both sections are made of a hard material. The machined material (chip) is simultaneously forced through an 'extrusion' die formed by the bottom rake face and the top constraining edge, thereby, effecting dimension and shape control. Microstructure refinement is effected by the strain imposed in the chip in the deformation zone, as in machining. The strain is determined by the tool rake angle and the deformation ratio [1].

Figure 2 shows foil, plate and bar samples of copper created by the LSEM process. The microstructure of the samples is ultrafine grained as determined by TEM. This demonstrates that significant shape change and control can be effected by LSEM while creating bulk nanostructured materials [1]. As in machining and other severe plastic deformation processes, the level of microstructure refinement increases with increasing strain. Similar nanostructured bulk forms have been created by this process out of CP-Ti, Al 6061-T6, Ta and Inconel 718. In all cases, the hardness and strength show enhancements commensurate with the microstructure refinement. Current work is aimed at scaling up the LSEM process to produce sheet samples several millimeters thick and tens of millimeters in length and width, for large-scale mechanical and wear testing

Problems Encountered

None

Status of Milestones

"Evaluate a range of consolidation and densification routes that enable bulk monolithic and composite materials to be produced from nanostructured machining chip particulate without significant coarsening." On schedule.

Publications

1) W. Moscoso, M. R. Shankar, J. B. Mann, W. D. Compton and S. Chandrasekar. Bulk nanostructured materials by large-strain extrusion machining. *Journal of Materials Research*, **22-1**, 201-205, 2007.

2) S. Swaminathan, M. Ravi Shankar, B. C. Rao, A. H. King, S. Chandrasekar, W. D. Compton and K. P. Trumble. Large strain deformation and nanostructured materials by machining, *Journal of Materials Science*, **42-5**, 1529-1541, 2007

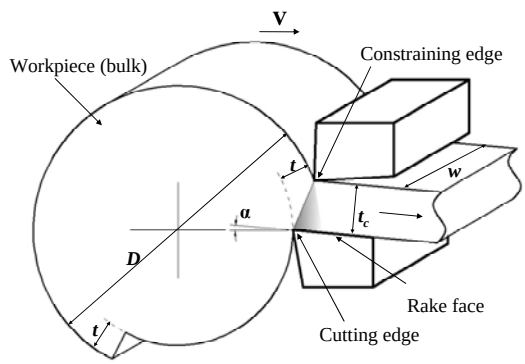

Figure 1 Schematic of Large Strain Extrusion Machining (LSEM).

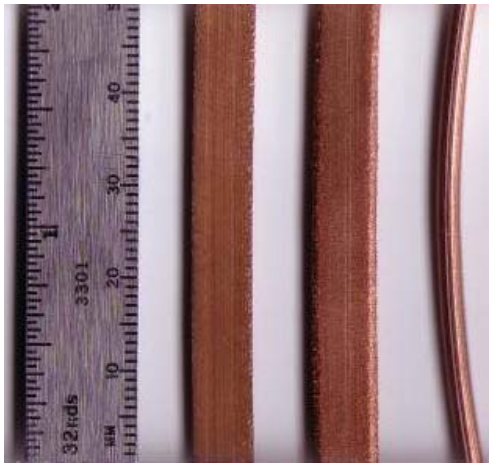

Figure 2 Examples of bulk forms of copper with UFG microstructure created by the LSEM process.

Modeling of Thermoelectrics

A. A. Wereszczak
Ceramic Science and Technology (CerSAT)
Oak Ridge National Laboratory

Objective/Scope

Potential next generation thermoelectric (TE) devices comprised of p- and n-type oxide ceramics enjoy strong interest for implementation in high temperature and oxidizing environments because their waste heat could be used to generate electricity. However, the intended TE function of these devices will only be enabled if the device is designed to overcome the thermomechanical limitations (i.e., brittleness) inherent to these oxides. A TE oxide with a combination of poor strength and low thermal conductivity can readily fail in the presence of a thermal gradient thereby preventing the exploitation of the desired thermoelectrical function.

This seemingly insurmountable problem can be overcome with the combined use of established probabilistic design methods developed for brittle structural components, good thermoelastic and thermomechanical databases of the candidate oxide material comprising the TE device, and iteratively applied design sensitivity analysis. This project executes this process by interrogating the reliability of prototypical TE devices (e.g., thin-film-based) and oxides.

There will be several outcomes from this work that will benefit TE oxide and device developers and end-users of these potentially high temperature TE devices: mechanical reliability of prototypical TE devices will be evaluated from a structural ceramic perspective and suggested redesigns will be identified, thermomechanical reliability of developmental TE oxides will be assessed, and minimum required thermomechanical properties of hypothetical TE oxides would be identified that produce desired reliability in a TE device. Additionally, innovative and cost-effective methods to process high temperature capable TEs will be a part of this project's research portfolio.

Technical Highlights

Finite element analysis (FEA) and probability design sensitivity (PDS) analysis of TE devices and their constituents are the primary efforts in this project. Two sets of input data are needed for their analyses.

> Thermoelastic Properties: Young's Modulus, Poisson's ratio, and the coefficient of thermal expansion as a function of temperature of each constituent's material. Anisotropy of those properties needs to be identified.
>
> Thermomechanical Properties: Flexure or tensile strength as a function of temperature of each constituent's material. Fractography on all biaxial flexure strength test coupons and identify failure initiation locations, and perform SEM fractography on selected specimens.

Literature values of the above, or estimated values if they are not available, are being used in these analyses.

Dr. O. M. Jadaan of the University of Wisconsin-Platteville will work with Wereszczak during the third and fourth quarters on these analyses. PDS analysis will be performed on a TE device and those materials properties (e.g., those listed above) whose control will have the largest effect on reliability will ranked.

Status of FY 2007 Milestones

Perform probability design sensitivity analysis on a TE device and rank those material properties or dimensions whose control would have the largest effect on reliability. **(Sep07)** *On schedule.*

Communications/Visits/Travel

Wereszczak participated in a conference call on February 01 with staff from General Motors, General Electric, the University of South Florida, and the University of Michigan.

Wereszczak visited General Electric (Niskayuna, NY) March 14 to meet with Todd Anderson, Kristin Brosnan, and Jie Jiang to talk about thermoelectric device modeling and issues associated with the mechanical properties needed for their design.

Publications

None.

References

None.